Rotational Spectroscopy of Diatomic Molecules

JOHN M. BROWN
Professor of Chemistry, University of Oxford
Fellow of Exeter College, Oxford

ALAN CARRINGTON
Former Royal Society Research Professor, Department of Chemistry,
University of Southampton
Honorary Fellow of Downing College, Cambridge

CAMBRIDGE
UNIVERSITY PRESS

PUBLISHED BY THE PRESS SYNDICATE OF THE UNIVERSITY OF CAMBRIDGE
The Pitt Building, Trumpington Street, Cambridge, United Kingdom

CAMBRIDGE UNIVERSITY PRESS
The Edinburgh Building, Cambridge CB2 2RU, UK
40 West 20th Street, New York, NY 10011-4211, USA
477 Williamstown Road, Port Melbourne, VIC 3207, Australia
Ruiz de Alarcón 13, 28014 Madrid, Spain
Dock House, The Waterfront, Cape Town 8001, South Africa

http://www.cambridge.org

© John Brown and Alan Carrington

This book is in copyright. Subject to statutory exception
and to the provisions of relevant collective licensing agreements,
no reproduction of any part may take place without
the written permission of Cambridge University Press.

First published 2003

Printed in the United Kingdom at the University Press, Cambridge

Typeface Times New Roman 10/13 pt and Scala Sans *System* LATEX 2_ε [TB]

A catalogue record for this book is available from the British Library

Library of Congress Cataloguing in Publication data

Brown, John M.
Rotational spectroscopy of diatomic molecules/John M. Brown, Alan Carrington.
p. cm. – (Cambridge molecular science)
Includes bibliographical references and index.
ISBN 0 521 81009 4 – ISBN 0 521 53078 4 (pb.)
1. Molecular spectroscopy. I. Carrington, Alan. II. Title. III. Series.
QC454.M6 B76 2003
539′.6′0287–dc21 2002073930

ISBN 0 521 81009 4 hardback
ISBN 0 521 53078 4 paperback

The publisher has used its best endeavours to ensure that the URLs for external websites referred to in this book are correct and active at the time of going to press. However, the publisher has no responsibility for the websites and can make no guarantee that a site will remain live or that the content is or will remain appropriate.

Contents

Preface *page* xv
Summary of notation xix
Figure acknowledgements xxiii

1 General introduction 1
1.1 Electromagnetic spectrum 1
1.2 Electromagnetic radiation 3
1.3 Intramolecular nuclear and electronic dynamics 5
1.4 Rotational levels 9
1.5 Historical perspectives 12
1.6 Fine structure and hyperfine structure of rotational levels 14
  1.6.1 Introduction 14
  1.6.2 $^1\Sigma^+$ states 15
  1.6.3 Open shell Σ states 21
  1.6.4 Open shell states with both spin and orbital angular momentum 26
1.7 The effective Hamiltonian 29
1.8 Bibliography 32
Appendix 1.1 Maxwell's equations 33
Appendix 1.2 Electromagnetic radiation 35
References 36

2 The separation of nuclear and electronic motion 38
2.1 Introduction 38
2.2 Electronic and nuclear kinetic energy 40
  2.2.1 Introduction 40
  2.2.2 Origin at centre of mass of molecule 41
  2.2.3 Origin at centre of mass of nuclei 43
  2.2.4 Origin at geometrical centre of the nuclei 44
2.3 The total Hamiltonian in field-free space 44
2.4 The nuclear kinetic energy operator 45
2.5 Transformation of the electronic coordinates to molecule-fixed axes 51
  2.5.1 Introduction 51
  2.5.2 Space transformations 52
  2.5.3 Spin transformations 54
2.6 Schrödinger equation for the total wave function 59
2.7 The Born–Oppenheimer and Born adiabatic approximations 60

2.8 Separation of the vibrational and rotational wave equations 61
2.9 The vibrational wave equation 63
2.10 Rotational Hamiltonian for space-quantised electron spin 67
2.11 Non-adiabatic terms 67
2.12 Effects of external electric and magnetic fields 68
Appendix 2.1 Derivation of the momentum operator 71
References 72

3 The electronic Hamiltonian 73
3.1 The Dirac equation 73
3.2 Solutions of the Dirac equation in field-free space 76
3.3 Electron spin magnetic moment and angular momentum 77
3.4 The Foldy–Wouthuysen transformation 80
3.5 The Foldy–Wouthuysen and Dirac representations for a free particle 85
3.6 Derivation of the many-electron Hamiltonian 89
3.7 Effects of applied static magnetic and electric fields 94
3.8 Retarded electromagnetic interaction between electrons 97
    3.8.1 Introduction 97
    3.8.2 Lorentz transformation 98
    3.8.3 Electromagnetic potentials due to a moving electron 99
    3.8.4 Gauge invariance 101
    3.8.5 Classical Lagrangian and Hamiltonian 103
3.9 The Breit Hamiltonian 104
    3.9.1 Introduction 104
    3.9.2 Reduction of the Breit Hamiltonian to non-relativistic form 105
3.10 Electronic interactions in the nuclear Hamiltonian 109
3.11 Transformation of coordinates in the field-free total Hamiltonian 110
3.12 Transformation of coordinates for the Zeeman and Stark terms in the total Hamiltonian 114
3.13 Conclusions 118
Appendix 3.1 Power series expansion of the transformed Hamiltonian 121
References 122

4 Interactions arising from nuclear magnetic and electric moments 123
4.1 Nuclear spins and magnetic moments 123
4.2 Derivation of nuclear spin magnetic interactions through the magnetic vector potential 125
4.3 Derivation of nuclear spin interactions from the Breit equation 130
4.4 Nuclear electric quadrupole interactions 131
    4.4.1 Spherical tensor form of the Hamiltonian operator 131
    4.4.2 Cartesian form of the Hamiltonian operator 133
    4.4.3 Matrix elements of the quadrupole Hamiltonian 134
4.5 Transformation of coordinates for the nuclear magnetic dipole and electric quadrupole terms 136
References 138

5 Angular momentum theory and spherical tensor algebra 139
5.1 Introduction 139
5.2 Rotation operators 140
  5.2.1 Introduction 140
  5.2.2 Decomposition of rotational operators 142
  5.2.3 Commutation relations 142
  5.2.4 Representations of the rotation group 143
  5.2.5 Orbital angular momentum and spherical harmonics 144
5.3 Rotations of a rigid body 146
  5.3.1 Introduction 146
  5.3.2 Rotation matrices 148
  5.3.3 Spin 1/2 systems 150
  5.3.4 Symmetric top wave functions 150
5.4 Addition of angular momenta 152
  5.4.1 Introduction 152
  5.4.2 Wigner 3-j symbols 154
  5.4.3 Coupling of three or more angular momenta: Racah algebra, Wigner 6-j and 9-j symbols 155
  5.4.4 Clebsch–Gordan series 157
  5.4.5 Integrals over products of rotation matrices 158
5.5 Irreducible spherical tensor operators 159
  5.5.1 Introduction 159
  5.5.2 Examples of spherical tensor operators 160
  5.5.3 Matrix elements of spherical tensor operators: the Wigner–Eckart theorem 163
  5.5.4 Matrix elements for composite systems 165
  5.5.5 Relationship between operators in space-fixed and molecule-fixed coordinate systems 167
  5.5.6 Treatment of the anomalous commutation relationships of rotational angular momenta by spherical tensor methods 168
Appendix 5.1 Summary of standard results from spherical tensor algebra 171
References 175

6 Electronic and vibrational states 177
6.1 Introduction 177
6.2 Atomic structure and atomic orbitals 178
  6.2.1 The hydrogen atom 178
  6.2.2 Many-electron atoms 181
  6.2.3 Russell–Saunders coupling 184
  6.2.4 Wave functions for the helium atom 187
  6.2.5 Many-electron wave functions: the Hartree–Fock equation 190
  6.2.6 Atomic orbital basis set 194
  6.2.7 Configuration interaction 196
6.3 Molecular orbital theory 197

6.4 Correlation of molecular and atomic electronic states 203
6.5 Calculation of molecular electronic wave functions and energies 206
  6.5.1 Introduction 206
  6.5.2 Electronic wave function for the H_2^+ molecular ion 207
  6.5.3 Electronic wave function for the H_2 molecule 208
  6.5.4 Many-electron molecular wave functions 212
6.6 Corrections to Born–Oppenheimer calculations for H_2^+ and H_2 219
6.7 Coupling of electronic and rotational motion: Hund's coupling cases 224
  6.7.1 Introduction 224
  6.7.2 Hund's coupling case (a) 225
  6.7.3 Hund's coupling case (b) 226
  6.7.4 Hund's coupling case (c) 228
  6.7.5 Hund's coupling case (d) 228
  6.7.6 Hund's coupling case (e) 229
  6.7.7 Intermediate coupling 230
  6.7.8 Nuclear spin coupling cases 232
6.8 Rotations and vibrations of the diatomic molecule 233
  6.8.1 The rigid rotor 233
  6.8.2 The harmonic oscillator 235
  6.8.3 The anharmonic oscillator 238
  6.8.4 The non-rigid rotor 242
  6.8.5 The vibrating rotor 243
6.9 Inversion symmetry of rotational levels 244
  6.9.1 The space-fixed inversion operator 244
  6.9.2 The effect of space-fixed inversion on the Euler angles and on molecule-fixed coordinates 245
  6.9.3 The transformation of general Hund's case (a) and case (b) functions under space-fixed inversion 246
  6.9.4 Parity combinations of basis functions 251
6.10 Permutation symmetry of rotational levels 251
  6.10.1 The nuclear permutation operator for a homonuclear diatomic molecule 251
  6.10.2 The transformation of general Hund's case (a) and case (b) functions under nuclear permutation P_{12} 252
  6.10.3 Nuclear statistical weights 254
6.11 Theory of transition probabilities 256
  6.11.1 Time-dependent perturbation theory 256
  6.11.2 The Einstein transition probabilities 258
  6.11.3 Einstein transition probabilities for electric dipole transitions 261
  6.11.4 Rotational transition probabilities 263
  6.11.5 Vibrational transition probabilities 266
  6.11.6 Electronic transition probabilities 267
  6.11.7 Magnetic dipole transition probabilities 269

6.12 Line widths and spectroscopic resolution 273
6.12.1 Natural line width 273
6.12.2 Transit time broadening 273
6.12.3 Doppler broadening 274
6.12.4 Collision broadening 275
6.13 Relationships between potential functions and the vibration–rotation levels 276
6.13.1 Introduction 276
6.13.2 The JWKB semiclassical method 277
6.13.3 Inversion of experimental data to calculate the potential function (RKR) 280
6.14 Long-range near-dissociation interactions 282
6.15 Predissociation 286
Appendix 6.1 Calculation of the Born–Oppenheimer potential for the H_2^+ ion 289
References 298

7 Derivation of the effective Hamiltonian 302
7.1 Introduction 302
7.2 Derivation of the effective Hamiltonian by degenerate perturbation theory: general principles 303
7.3 The Van Vleck and contact transformations 312
7.4 Effective Hamiltonian for a diatomic molecule in a given electronic state 316
7.4.1 Introduction 316
7.4.2 The rotational Hamiltonian 319
7.4.3 Hougen’s isomorphic Hamiltonian 320
7.4.4 Fine structure terms: spin–orbit, spin–spin and spin–rotation operators 323
7.4.5 Λ-doubling terms for a Π electronic state 328
7.4.6 Nuclear hyperfine terms 331
7.4.7 Higher-order fine structure terms 335
7.5 Effective Hamiltonian for a single vibrational level 338
7.5.1 Vibrational averaging and centrifugal distortion corrections 338
7.5.2 The form of the effective Hamiltonian 341
7.5.3 The $\boldsymbol{N}^2$ formulation of the effective Hamiltonian 343
7.5.4 The isotopic dependence of parameters in the effective Hamiltonian 344
7.6 Effective Zeeman Hamiltonian 347
7.7 Indeterminacies: rotational contact transformations 352
7.8 Estimates and interpretation of parameters in the effective Hamiltonian 356
7.8.1 Introduction 356
7.8.2 Rotational constant 356
7.8.3 Spin–orbit coupling constant, A 357
7.8.4 Spin–spin and spin–rotation parameters, λ and γ 360

7.8.5 Λ-doubling parameters 362
7.8.6 Magnetic hyperfine interactions 363
7.8.7 Electric quadrupole hyperfine interaction 365
Appendix 7.1 Molecular parameters or constants 368
References 369

8 Molecular beam magnetic and electric resonance 371
8.1 Introduction 371
8.2 Molecular beam magnetic resonance of closed shell molecules 372
8.2.1 H_2, D_2 and HD in their $X\,{}^1\Sigma^+$ ground states 372
8.2.2 Theory of Zeeman interactions in ${}^1\Sigma^+$ states 390
8.2.3 Na_2 in the $X\,{}^1\Sigma_g^+$ ground state: optical state selection and detection 416
8.2.4 Other ${}^1\Sigma^+$ molecules 421
8.3 Molecular beam magnetic resonance of electronically excited molecules 422
8.3.1 H_2 in the $c\,{}^3\Pi_u$ state 422
8.3.2 N_2 in the $A\,{}^3\Sigma_u^+$ state 446
8.4 Molecular beam electric resonance of closed shell molecules 463
8.4.1 Principles of electric resonance methods 463
8.4.2 CsF in the $X\,{}^1\Sigma^+$ ground state 465
8.4.3 LiBr in the $X\,{}^1\Sigma^+$ ground state 483
8.4.4 Alkaline earth and group IV oxides 487
8.4.5 HF in the $X\,{}^1\Sigma^+$ ground state 489
8.4.6 HCl in the $X\,{}^1\Sigma^+$ ground state 500
8.5 Molecular beam electric resonance of open shell molecules 508
8.5.1 Introduction 508
8.5.2 LiO in the $X\,{}^2\Pi$ ground state 509
8.5.3 NO in the $X\,{}^2\Pi$ ground state 526
8.5.4 OH in the $X\,{}^2\Pi$ ground state 538
8.5.5 CO in the $a\,{}^3\Pi$ state 552
Appendix 8.1 Nuclear spin dipolar interaction 558
Appendix 8.2 Relationship between the cartesian and spherical tensor forms of the electron spin–nuclear spin dipolar interaction 561
Appendix 8.3 Electron spin–electron spin dipolar interaction 563
Appendix 8.4 Matrix elements of the quadrupole Hamiltonian 568
Appendix 8.5 Magnetic hyperfine Hamiltonian and hyperfine constants 573
References 574

9 Microwave and far-infrared magnetic resonance 579
9.1 Introduction 579
9.2 Experimental methods 579
9.2.1 Microwave magnetic resonance 579
9.2.2 Far-infrared laser magnetic resonance 584
9.3 ${}^1\Delta$ states 587
9.3.1 SO in the $a\,{}^1\Delta$ state 587
9.3.2 NF in the $a\,{}^1\Delta$ state 591

9.4 $^2\Pi$ states 596
    9.4.1 Introduction 596
    9.4.2 ClO in the $X\,^2\Pi$ ground state 597
    9.4.3 OH in the $X\,^2\Pi$ ground state 613
    9.4.4 Far-infrared laser magnetic resonance of CH in the $X\,^2\Pi$ ground state 624
9.5 $^2\Sigma$ states 633
    9.5.1 Introduction 633
    9.5.2 CN in the $X\,^2\Sigma^+$ ground state 633
9.6 $^3\Sigma$ states 641
    9.6.1 SO in the $X\,^3\Sigma^-$ ground state 641
    9.6.2 SeO in the $X\,^3\Sigma^-$ ground state 649
    9.6.3 NH in the $X\,^3\Sigma^-$ ground state 652
9.7 $^3\Pi$ states 655
    9.7.1 CO in the $a\,^3\Pi$ state 655
9.8 $^4\Sigma$ states 661
    9.8.1 CH in the $a\,^4\Sigma^-$ state 661
9.9 $^4\Delta$, $^3\Phi$, $^2\Delta$ and $^6\Sigma^+$ states 665
    9.9.1 Introduction 665
    9.9.2 CrH in the $X\,^6\Sigma^+$ ground state 666
    9.9.3 FeH in the $X\,^4\Delta$ ground state 669
    9.9.4 CoH in the $X\,^3\Phi$ ground state 669
    9.9.5 NiH in the $X\,^2\Delta$ ground state 674
Appendix 9.1 Evaluation of the reduced matrix element of $\mathrm{T}^3(\boldsymbol{S}, \boldsymbol{S}, \boldsymbol{S})$ 678
References 680

10 Pure rotational spectroscopy 683
10.1 Introduction and experimental methods 683
    10.1.1 Simple absorption spectrograph 683
    10.1.2 Microwave radiation sources 685
    10.1.3 Modulation spectrometers 688
    10.1.4 Superheterodyne detection 701
    10.1.5 Fourier transform spectrometer 703
    10.1.6 Radio telescopes and radio astronomy 713
    10.1.7 Terahertz (far-infrared) spectrometers 723
    10.1.8 Ion beam techniques 728
10.2 $^1\Sigma^+$ states 732
    10.2.1 CO in the $X\,^1\Sigma^+$ ground state 732
    10.2.2 HeH^+ in the $X\,^1\Sigma^+$ ground state 736
    10.2.3 CuCl and CuBr in their $X\,^1\Sigma^+$ ground states 738
    10.2.4 SO, NF and NCl in their $b\,^1\Sigma^+$ states 741
    10.2.5 Hydrides (LiH, NaH, KH, CuH, AlH, AgH) in their $X\,^1\Sigma^+$ ground states 743

10.3 $^2\Sigma$ states 745
  10.3.1 CO^+ in the $X\,^2\Sigma^+$ ground state 745
  10.3.2 CN in the $X\,^2\Sigma^+$ ground state 749
10.4 $^3\Sigma$ states 752
  10.4.1 Introduction 752
  10.4.2 O_2 in its $X\,^3\Sigma_g^-$ ground state 754
  10.4.3 SO, S_2 and NiO in their $X\,^3\Sigma^-$ ground states 759
  10.4.4 PF, NCl, NBr and NI in their $X\,^3\Sigma^-$ ground states 763
10.5 $^1\Delta$ states 776
  10.5.1 O_2 in its $a\,^1\Delta_g$ state 776
  10.5.2 SO and NCl in their $a\,^1\Delta$ states 779
10.6 $^2\Pi$ states 782
  10.6.1 NO in the $X\,^2\Pi$ ground state 782
  10.6.2 OH in the $X\,^2\Pi$ ground state 788
  10.6.3 CH in the $X\,^2\Pi$ ground state 794
  10.6.4 CF, SiF, GeF in their $X\,^2\Pi$ ground states 810
  10.6.5 Other free radicals with $^2\Pi$ ground states 811
10.7 Case (c) doublet state molecules 813
  10.7.1 Studies of the $HeAr^+$ ion 813
  10.7.2 Studies of the $HeKr^+$ ion 832
10.8 Higher spin/orbital states 834
  10.8.1 CO in the $a\,^3\Pi$ state 834
  10.8.2 SiC in the $X\,^3\Pi$ ground state 836
  10.8.3 FeC in the $X\,^3\Delta$ ground state 841
  10.8.4 VO and NbO in their $X\,^4\Sigma^-$ ground states 841
  10.8.5 FeF and FeCl in their $X\,^6\Delta$ ground states 845
  10.8.6 CrF, CrCl and MnO in their $X\,^6\Sigma^+$ ground states 850
  10.8.7 FeO in the $X\,^5\Delta$ ground state 853
  10.8.8 TiCl in the $X\,^4\Phi$ ground state 854
10.9 Observation of a pure rotational transition in the H_2^+ molecular ion 856
References 862

11 Double resonance spectroscopy 870
11.1 Introduction 870
11.2 Radiofrequency and microwave studies of CN in its excited electronic states 871
11.3 Early radiofrequency or microwave/optical double resonance studies 876
  11.3.1 Radiofrequency/optical double resonance of CS in its excited $A\,^1\Pi$ state 876
  11.3.2 Radiofrequency/optical double resonance of OH in its excited $A\,^2\Sigma^+$ state 880
  11.3.3 Microwave/optical double resonance of BaO in its ground $X\,^1\Sigma^+$ and excited $A\,^1\Sigma^+$ states 883

11.4 Microwave/optical magnetic resonance studies of electronically excited H_2 885
  11.4.1 Introduction 885
  11.4.2 H_2 in the $G\ ^1\Sigma_g^+$ state 885
  11.4.3 H_2 in the $d\ ^3\Pi_u$ state 892
  11.4.4 H_2 in the $k\ ^3\Pi_u$ state 900
11.5 Radiofrequency or microwave/optical double resonance of alkaline earth molecules 902
  11.5.1 Introduction 902
  11.5.2 SrF, CaF and CaCl in their $X\ ^2\Sigma^+$ ground states 902
11.6 Radiofrequency or microwave/optical double resonance of transition metal molecules 906
  11.6.1 Introduction 906
  11.6.2 FeO in the $X\ ^5\Delta$ ground state 909
  11.6.3 CuF in the $b\ ^3\Pi$ excited state 913
  11.6.4 CuO in the $X\ ^2\Pi$ ground state 917
  11.6.5 ScO in the $X\ ^2\Sigma^+$ ground state 919
  11.6.6 TiO in the $X\ ^3\Delta$ ground state and TiN in the $X\ ^2\Sigma^+$ ground state 922
  11.6.7 CrN and MoN in their $X\ ^4\Sigma^-$ ground states 924
  11.6.8 NiH in the $X\ ^2\Delta$ ground state 927
  11.6.9 4*d* transition metal molecules: YF in the $X\ ^1\Sigma^+$ ground state, YO and YS in their $X\ ^2\Sigma^+$ ground states 930
11.7 Microwave/optical double resonance of rare earth molecules 936
  11.7.1 Radiofrequency/optical double resonance of YbF in its $X\ ^2\Sigma^+$ ground state 936
  11.7.2 Radiofrequency/optical double resonance of LaO in its $X\ ^2\Sigma^+$ and $B\ ^2\Sigma^+$ states 938
11.8 Double resonance spectroscopy of molecular ion beams 942
  11.8.1 Radiofrequency and microwave/infrared double resonance of HD^+ in the $X\ ^2\Sigma^+$ ground state 942
  11.8.2 Radiofrequency/optical double resonance of N_2^+ in the $X\ ^2\Sigma_g^+$ ground state 953
  11.8.3 Microwave/optical double resonance of CO^+ in the $X\ ^2\Sigma^+$ ground state 958
11.9 Quadrupole trap radiofrequency spectroscopy of the H_2^+ ion 960
  11.9.1 Introduction 960
  11.9.2 Principles of photo-alignment 960
  11.9.3 Experimental methods and results 962
  11.9.4 Analysis of the spectra 964
  11.9.5 Quantitative interpretation of the molecular parameters 972
References 974

General appendices 978
Appendix A Values of the fundamental constants 978

Appendix B Selected set of nuclear properties for naturally occurring isotopes 979
Appendix C Compilation of Wigner 3-j symbols 987
Appendix D Compilation of Wigner 6-j symbols 991
Appendix E Relationships between cgs and SI units 993

Author index 994
Subject index 1004

1 General introduction

1.1. Electromagnetic spectrum

Molecular spectroscopy involves the study of the absorption or emission of electromagnetic radiation by matter; the radiation may be detected directly, or indirectly through its effects on other molecular properties. The primary purpose of spectroscopic studies is to understand the nature of the nuclear and electronic motions within a molecule.

The different branches of spectroscopy may be classified either in terms of the wavelength, or frequency, of the electromagnetic radiation, or in terms of the type of intramolecular dynamic motion primarily involved. Historically the first method has been the most common, with different regions of the electromagnetic spectrum classified as shown in figure 1.1. In the figure we show four different ways of describing these regions. They may be classified according to the wavelength, in ångström units ($1\,\text{Å} = 10^{-8}$ cm), or the frequency in Hz; wavelength (λ) and frequency (ν) are related by the equation,

$$\nu = c/\lambda, \tag{1.1}$$

where c is the speed of light. Very often the wavenumber unit, cm^{-1}, is used; we denote this by the symbol $\tilde{\nu}$. Clearly the wavelength and wavenumber are related in the simple way

$$\tilde{\nu} = 1/\lambda, \tag{1.2}$$

with λ expressed in cm. Although offensive to the purist, the wavenumber is often taken as a unit of energy, according to the Planck relationship

$$E = h\nu = hc\tilde{\nu}, \tag{1.3}$$

where h is Planck's constant. From the values of the fundamental constants given in General Appendix A, we find that 1 cm^{-1} corresponds to $1.986\,445 \times 10^{-23}$ J molecule^{-1}. A further unit of energy which is often used, and which will appear in this book, is the electronvolt, eV; this is the kinetic energy of an electron which has been accelerated through a potential difference of 1 V; 1 eV is equal to 8065.545 cm^{-1}.

In the classical theory of electrodynamics, electromagnetic radiation is emitted when an electron moves in its orbit but, according to the Bohr theory of the atom,

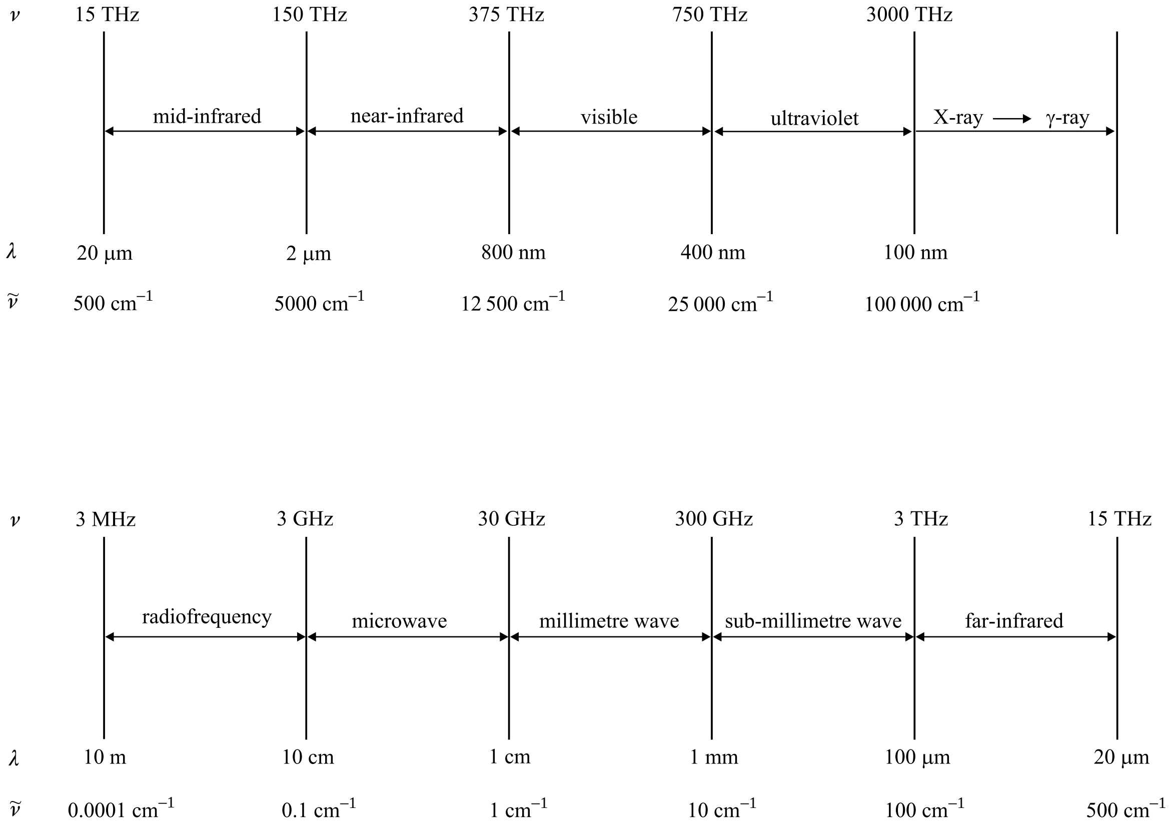
ν
15 THz
150 THz
375 THz
750 THz
3000 THz
mid-infrared
near-infrared
visible
ultraviolet
X-ray → γ-ray
λ
20 µm
2 µm
800 nm
400 nm
100 nm
ν̃
500 cm⁻¹
5000 cm⁻¹
12 500 cm⁻¹
25 000 cm⁻¹
100 000 cm⁻¹
ν
3 MHz
3 GHz
30 GHz
300 GHz
3 THz
15 THz
radiofrequency
microwave
millimetre wave
sub-millimetre wave
far-infrared
λ
10 m
10 cm
1 cm
1 mm
100 µm
20 µm
ν̃
0.0001 cm⁻¹
0.1 cm⁻¹
1 cm⁻¹
10 cm⁻¹
100 cm⁻¹
500 cm⁻¹

Figure 1.1. The electromagnetic spectrum, classified according to frequency (ν), wavelength (λ), and wavenumber units ($\tilde{\nu}$). There is no established convention for the division of the spectrum into different regions; we show our convention.

emission of radiation occurs only when an electron goes from a higher energy orbit E_2 to an orbit of lower energy E_1. The emitted energy is a photon of energy $h\nu$, given by

$$h\nu = E_2 - E_1, \tag{1.4}$$

an equation known as the Bohr frequency condition. The reverse process, a transition from E_1 to E_2, requires the absorption of a quantum of energy $h\nu$. The range of frequencies (or energies) which constitutes the electromagnetic spectrum is shown in figure 1.1. Molecular spectroscopy covers a nominal energy range from 0.0001 cm^{-1} to 100 000 cm^{-1}, that is, nine decades in energy, frequency or wavelength. The spectroscopy described in this book, which we term *rotational* spectroscopy for reasons to be given later, is concerned with the range 0.0001 cm^{-1} to 100 cm^{-1}. Surprisingly, therefore, it covers six of the nine decades shown in figure 1.1, very much the major portion of the molecular spectrum! Indeed our low frequency cut-off at 3 MHz is somewhat arbitrary, since molecular beam magnetic resonance studies at even lower frequencies have been described. As we shall see, the experimental techniques employed over the full range given in figure 1.1 vary a great deal. We also note here that the spectroscopy discussed in this book is concerned solely with molecules in the gas phase. Again the reasons for this discrimination will become apparent later in this chapter.

So far as the classification of the type of spectroscopy performed is concerned, the characterisation of the dynamical motions of the nuclei and electrons within a molecule is more important than the region of the electromagnetic spectrum in which the corresponding transitions occur. However, before we come to this in more detail, a brief discussion of the nature of electromagnetic radiation is necessary. This is actually a huge subject which, if tackled properly, takes us deeply into the details of classical and semiclassical electromagnetism, and even further into quantum electrodynamics. The basic foundations of the subject are Maxwell's equations, which we describe in appendix 1.1. We will make use of the results of these equations in the next section, referring the reader to the appendix if more detail is required.

1.2. Electromagnetic radiation

Electromagnetic radiation consists of both an electric and a magnetic component, which for plane-polarised (or linearly-polarised) radiation, travelling along the Y axis, may be represented as shown in figure 1.2. Each of the three diagrams represents the electric and magnetic fields at different instants of time as indicated. The electric field ($\boldsymbol{E}$) is in the YZ plane parallel to the Z axis, and the magnetic field ($\boldsymbol{B}$) is everywhere perpendicular to the electric field, and therefore in the XY plane. Consideration of Maxwell's equations [1] shows that, as time progresses, the entire field pattern shifts to the right along the Y axis, with a velocity c. The wavelength of the radiation, λ, shown in the figure, is related to the frequency ν by the simple expression $\nu = c/\lambda$. At every point in the wave at any instant of time, the electric and magnetic field strengths

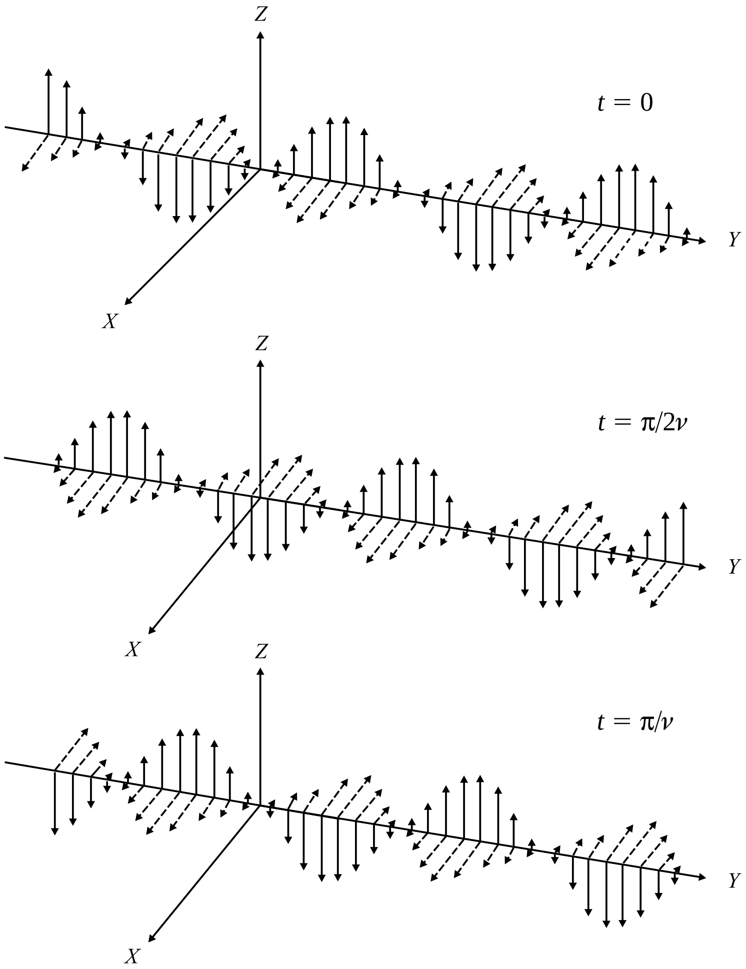

Figure 1.2. Schematic representation of plane-polarised radiation projected along the Y axis at three different instants of time. The solid arrows denote the amplitude of the electric field ($\boldsymbol{E}$), and the dashed arrows denote the perpendicular magnetic field ($\boldsymbol{B}$).

are equal; this means that, in cgs units, if the electric field strength is $10\,\mathrm{V\,cm^{-1}}$ the magnetic field strength is 10 G.

Although it is simplest to describe and represent graphically the example of plane polarised radiation, it is also instructive to consider the more general case [2]. For propagation of the radiation along the Y axis, the electric field $\boldsymbol{E}$ can be decomposed into components along the Z and X axes. The electric field vector in the XZ plane is then given by

$$\boldsymbol{E} = \boldsymbol{i}'E_X + \boldsymbol{k}'E_Z \tag{1.5}$$

where $\boldsymbol{i}'$ and $\boldsymbol{k}'$ are unit vectors along the X and Z axes. The components in equation (1.5) are given by

$$\begin{aligned} E_X &= E_X^0 \cos(k^* Y - \omega t + \alpha_X), \\ E_Z &= E_Z^0 \cos(k^* Y - \omega t + \alpha_Z), \\ \alpha &= \alpha_X - \alpha_Z. \end{aligned} \tag{1.6}$$

Here $\omega = 2\pi\nu$, ω is the angular frequency in units of rad s^{-1}, ν is the frequency in Hz, and $\boldsymbol{k}^*$ is called the propagation vector with units of inverse length. In a vacuum $\boldsymbol{k}^*$ has a magnitude equal to $2\pi/\lambda_0$ where λ_0 is the vacuum wavelength of the radiation. Finally, α is the difference in phase between the X and Z components of $\boldsymbol{E}$.

Plane-polarised radiation is obtained when the phase factor α is equal to 0 or π and $E_X^0 = E_Z^0$. When $\alpha = 0$, E_X and E_Z are in phase, whilst for $\alpha = \pi$ they are out-of-phase by π. The special case illustrated in figure 1.2 corresponds to $E_X^0 = 0$. Other forms of polarisation can be obtained from equations (1.6). For elliptically-polarised radiation we set $\alpha = \pm\pi/2$ so that equations (1.6) become

$$\begin{aligned} E_X &= E_X^0 \cos(k^* Y - \omega t), \\ E_Z &= E_Z^0 \cos(k^* Y - \omega t \pm \pi/2) = \pm E_Z^0 \sin(k^* Y - \omega t), \\ \boldsymbol{E}_\pm &= \boldsymbol{i}' E_X \pm \boldsymbol{k}' E_Z \\ &= \boldsymbol{i}' E_X^0 \cos(k^* Y - \omega t) \pm \boldsymbol{k}' E_Z^0 \sin(k^* Y - \omega t). \end{aligned} \tag{1.7}$$

If $E_X^0 = E_Z^0 = \mathcal{E}$ for $\alpha = \pm\pi/2$, we have circularly-polarised radiation given by the expression

$$E_\pm = \mathcal{E}[\boldsymbol{i}' \cos(k^* Y - \omega t) \pm \boldsymbol{k}' \sin(k^* Y - \omega t)]. \tag{1.8}$$

When viewed looking back along the Y axis towards the radiation source, the field rotates clockwise or counter clockwise about the Y axis. When $\alpha = +\pi/2$ which corresponds to E_+, the field appears to rotate counter clockwise about Y.

Conventional sources of electromagnetic radiation are incoherent, which means that the waves associated with any two photons of the same wavelength are, in general, out-of-phase and have a random phase relation with each other. Laser radiation, however, has both spatial and temporal coherence, which gives it special importance for many applications.

1.3. Intramolecular nuclear and electronic dynamics

In order to understand molecular energy levels, it is helpful to partition the kinetic energies of the nuclei and electrons in a molecule into parts which, if possible, separately represent the electronic, vibrational and rotational motions of the molecule. The details of the processes by which this partitioning is achieved are presented in chapter 2. Here we give a summary of the main procedures and results.

We start by writing a general expression which represents the kinetic energies of the nuclei (α) and electrons (i) in a molecule:

$$T = \sum_{\alpha} \frac{1}{2M_{\alpha}} \boldsymbol{P}_{\alpha}^{2} + \sum_{i} \frac{1}{2m} \boldsymbol{P}_{i}^{2}, \tag{1.9}$$

where M_{α} and m are the masses of the nuclei and electrons respectively. The momenta $\boldsymbol{P}_{\alpha}$ and $\boldsymbol{P}_{i}$ are vector quantities, which are defined by

$$\begin{aligned} \boldsymbol{P}_{i} &= -\mathrm{i}\hbar \frac{\partial}{\partial \boldsymbol{R}_{i}}, \\ \boldsymbol{P}_{\alpha} &= -\mathrm{i}\hbar \frac{\partial}{\partial \boldsymbol{R}_{\alpha}}, \end{aligned} \tag{1.10}$$

expressed in a space-fixed axis system (X, Y, Z) of arbitrary origin. $\boldsymbol{R}_{\alpha}$ gives the position of nucleus α within this coordinate system. The partial derivative $(\partial/\partial \boldsymbol{R}_{\alpha})$ is a shorthand notation for the three components of the gradient operator,

$$\frac{\partial}{\partial \boldsymbol{R}_{\alpha}} \equiv \left(\frac{\partial}{\partial R_{X}}\right)_{\alpha} \boldsymbol{i}' + \left(\frac{\partial}{\partial R_{Y}}\right)_{\alpha} \boldsymbol{j}' + \left(\frac{\partial}{\partial R_{Z}}\right)_{\alpha} \boldsymbol{k}', \tag{1.11}$$

where $\boldsymbol{i}'$, $\boldsymbol{j}'$, $\boldsymbol{k}'$ are unit vectors along the space-fixed axes X, Y, Z.

It is by no means obvious that (1.9) contains the vibrational and rotational motion of the nuclei, as well as the electron kinetic energies, but a series of origin and axis transformations shows that this is the case. First, we transform from the arbitrary origin to an origin at the centre of mass of the molecule, and then to the centre of mass of the nuclei. As we show in chapter 2, these transformations convert (1.9) into the expression

$$T = \frac{1}{2M} \boldsymbol{P}_{\mathrm{O}}^{2} + \frac{1}{2\mu} \boldsymbol{P}_{R}^{2} + \frac{1}{2m} \sum_{i} \boldsymbol{P}_{i}^{\prime\prime 2} + \frac{1}{2(M_{1}+M_{2})} \sum_{i,j} \boldsymbol{P}_{i}^{\prime\prime} \cdot \boldsymbol{P}_{j}^{\prime\prime}. \tag{1.12}$$

The first term in (1.12) represents the kinetic energy due to translation of the whole molecule through space; this motion can be separated off rigorously in the absence of external fields. In the second term, μ is the reduced nuclear mass, $M_{1}M_{2}/(M_{1}+M_{2})$, and this term represents the kinetic energy of the nuclei. The third term describes the kinetic energy of the electrons and the last term is a correction term, known as the mass polarisation term. The transformation is described in detail in chapter 2 and appendix 2.1. An alternative expression equivalent to (1.12) is obtained by writing the momentum operators in terms of the Laplace operators,

$$T = -\frac{\hbar^{2}}{2M} \nabla^{2} - \frac{\hbar^{2}}{2\mu} \nabla_{R}^{2} - \frac{\hbar^{2}}{2m} \sum_{i} \nabla_{i}^{\prime\prime 2} - \frac{\hbar^{2}}{2(M_{1}+M_{2})} \sum_{i,j} \nabla_{i}^{\prime\prime} \cdot \nabla_{j}^{\prime\prime}. \tag{1.13}$$

The next step is to add terms representing the potential energy, the electron spin interactions and the nuclear spin interactions. The total Hamiltonian $\mathcal{H}_{\mathrm{T}}$ can then be subdivided into electronic and nuclear Hamiltonians,

$$\mathcal{H}_{\mathrm{T}} = \mathcal{H}_{\mathrm{el}} + \mathcal{H}_{\mathrm{nucl}}, \tag{1.14}$$

where

$$\mathcal{H}_{\rm el} = -\frac{\hbar^2}{2m}\sum_i \nabla_i^2 - \frac{\hbar^2}{2M_N}\sum_{i,j}\nabla_i \cdot \nabla_j + \sum_{i<j}\frac{e^2}{4\pi\varepsilon_0 R_{ij}} - \sum_{\alpha,i}\frac{Z_\alpha e^2}{4\pi\varepsilon_0 R_{i\alpha}} + \mathcal{H}(\boldsymbol{S}_i) + \mathcal{H}(\boldsymbol{I}_\alpha), \tag{1.15}$$

$$\mathcal{H}_{\rm nucl} = -\frac{\hbar^2}{2\mu}\nabla_R^2 + \sum_{\alpha,\beta}\frac{Z_\alpha Z_\beta e^2}{4\pi\varepsilon_0 R}. \tag{1.16}$$

The third and fourth terms in (1.15) represent the potential energy contributions (in SI units, see General Appendix E) arising from the electron–electron and electron–nuclear interactions, whilst the second term in (1.16) describes the nuclear repulsion term between nuclei with charges $Z_\alpha e$ and $Z_\beta e$. The electron and nuclear spin Hamiltonians introduced into (1.15) are described in detail later.

The total nuclear kinetic energy is contained within the first term in equation (1.16) and we now introduce a further transformation from the axes translating with the molecule but with fixed orientation to molecule-fixed axes gyrating with the nuclei. In chapter 2 the two axis systems are related by Euler angles, ϕ, θ and χ, although for diatomic molecules the angle χ is redundant. We may use a simpler transformation to spherical polar coordinates R, θ, ϕ as defined in figure 1.3. With this transformation the space-fixed coordinates are given by

$$\begin{aligned} X &= R\sin\theta\cos\phi, \\ Y &= R\sin\theta\sin\phi, \\ Z &= R\cos\theta. \end{aligned} \tag{1.17}$$

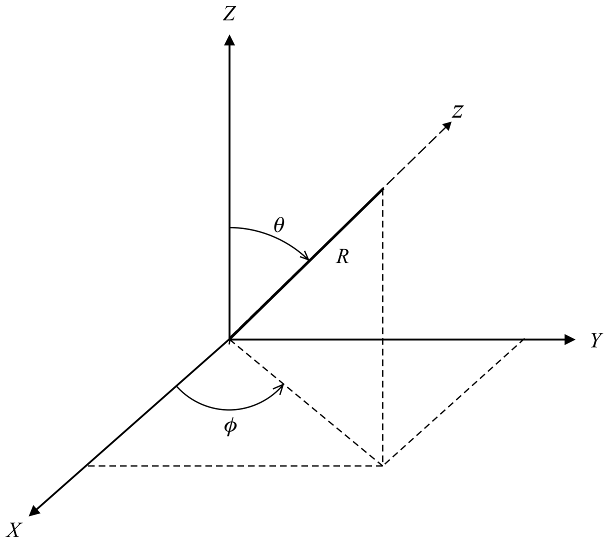

Figure 1.3. Transformation from space-fixed axes X, Y, Z to molecule-fixed axes using the spherical polar coordinates R, θ, ϕ, defined in the figure.

We proceed to show, in chapter 2, that this transformation of the axes leads to the nuclear kinetic energy term being converted into a new expression:

$$\begin{aligned}\frac{1}{2\mu}\boldsymbol{P}_R^2 &= -\frac{\hbar^2}{2\mu}\nabla_R^2 \\ &= -\frac{\hbar^2}{2\mu}\left\{\frac{1}{R^2}\frac{\partial}{\partial R}\left(R^2\frac{\partial}{\partial R}\right)+\frac{1}{R^2\sin\theta}\frac{\partial}{\partial\theta}\left(\sin\theta\frac{\partial}{\partial\theta}\right)+\frac{1}{R^2\sin^2\theta}\frac{\partial^2}{\partial\phi^2}\right\}.\end{aligned} \tag{1.18}$$

This is a very important result because the first term describes the vibrational kinetic energy of the nuclei, whilst the second and third terms represent the rotational kinetic energy. The transformation is straightforward provided one takes proper note of the non-commutation of the operator products which arise.

The transformation of terms representing the kinetic energies of all the particles into terms representing, separately, the electronic, vibrational and rotational kinetic energies is clearly very important. The nuclear kinetic energy Hamiltonian, (1.18), is relatively simple when the spherical polar coordinate transformation (1.17) is used. When the Euler angle transformation is used, it is a little more complicated, containing terms which include the third angle χ:

$$\begin{aligned}\mathcal{H}_{\text{nucl}} = &-\frac{\hbar^2}{2\mu R^2}\left\{\frac{\partial}{\partial R}\left(R^2\frac{\partial}{\partial R}\right)+\operatorname{cosec}\theta\frac{\partial}{\partial\theta}\left(\sin\theta\frac{\partial}{\partial\theta}\right)\right. \\ &\left.+\operatorname{cosec}^2\theta\left[\frac{\partial^2}{\partial\phi^2}+\frac{\partial^2}{\partial\chi^2}-2\cos\theta\frac{\partial^2}{\partial\phi\partial\chi}\right]\right\}+V_{\text{nucl}}(R).\end{aligned} \tag{1.19}$$

We show in chapter 2 that when the transformation of the electronic coordinates, including electron spin, into the rotating molecule-fixed axes system is taken into account, equation (1.19) takes the much simpler form

$$\mathcal{H}_{\text{nucl}} = -\frac{\hbar^2}{2\mu R^2}\frac{\partial}{\partial R}\left(R^2\frac{\partial}{\partial R}\right)+\frac{\hbar^2}{2\mu R^2}(\boldsymbol{J}-\boldsymbol{P})^2+V_{\text{nucl}}(R), \tag{1.20}$$

where $\boldsymbol{J}$ is the total angular momentum and $\boldsymbol{P}$ is the total electronic angular momentum, equal to $\boldsymbol{L}+\boldsymbol{S}$. Hence although the electronic Hamiltonian is free of terms involving the motion of the nuclei, the nuclear Hamiltonian (1.20) contains terms involving the operators P_x, P_y and P_z which operate on the electronic part of the total wave function. The Schrödinger equation for the total wave function is written as

$$(\mathcal{H}_{\text{el}}+\mathcal{H}_{\text{nucl}})\Psi_{\text{rve}} = E_{\text{rve}}\Psi_{\text{rve}}, \tag{1.21}$$

and, as we show in chapter 2, the Born approximation allows us to assume total wave functions of the form

$$\Psi_{\text{rve}}^0 = \psi_{\text{e}}^{\text{n}}(\boldsymbol{r}_i)\phi_{\text{rv}}^{\text{n}}(R,\phi,\theta). \tag{1.22}$$

The matrix elements of the nuclear Hamiltonian that mix different electronic states are then neglected; the electronic wave function is taken to be dependent upon nuclear coordinates, but not nuclear momenta. If the first-order contributions of the nuclear kinetic energy are taken into account, we have the Born adiabatic approximation; if they are neglected, we have the Born–Oppenheimer approximation. This approximation occupies a central position in molecular quantum mechanics; in most situations it is a good approximation, and allows us to proceed with concepts like the potential energy curve or surface, molecular shapes and geometry, etc. Those special cases, usually involving electronic orbital degeneracy, where the Born–Oppenheimer approximation breaks down, can often be treated by perturbation methods.

In chapter 2 we show how a separation of the vibrational and rotational wave functions can be achieved by using the product functions

$$\phi^{\mathrm{n}}_{\mathrm{r}v} = \chi^{\mathrm{n}}(R)\mathrm{e}^{\mathrm{i}M_J\phi}\Theta^{\mathrm{n}}(\theta)\mathrm{e}^{\mathrm{i}k\chi}, \tag{1.23}$$

where M_J and k are constants taking integral or half-odd values. We show that in the Born approximation, the wave equation for the nuclear wave functions can be expressed in terms of two equations describing the vibrational and rotational motion separately. Ultimately we obtain the wave equation of the vibrating rotator,

$$\frac{\hbar^2}{2\mu R^2}\frac{\partial}{\partial R}R^2\frac{\partial\chi^{\mathrm{n}}(R)}{\partial R} + \left\{E_{\mathrm{r}v\mathrm{e}} - V - \frac{\hbar^2}{2\mu R^2}J(J+1)\right\}\chi^{\mathrm{n}}(R) = 0. \tag{1.24}$$

The main problem with this equation is the description of the potential energy term (V). As we shall see, insertion of a restricted form of the potential allows one to express data on the ro-vibrational levels in terms of semi-empirical constants. If the Morse potential is used, the ro-vibrational energies are given by the expression

$$\begin{aligned} E_{v,J} = {} & \omega_e(v+1/2) - \omega_e x_e(v+1/2)^2 + B_e\,J(J+1) - D_e\,J^2(J+1)^2 \\ & - \alpha_e(v+1/2)J(J+1). \end{aligned} \tag{1.25}$$

The first two terms describe the vibrational energy, the next two the rotational energy, and the final term describes the vibration–rotation interaction.

1.4. Rotational levels

This book is concerned primarily with the rotational levels of diatomic molecules. The spectroscopic transitions described arise either from transitions between different rotational levels, usually adjacent rotational levels, or from transitions between the fine or hyperfine components of a single rotational level. The electronic and vibrational quantum numbers play a different role. In the majority of cases the rotational levels studied belong to the lowest vibrational level of the ground electronic state. The detailed nature of the rotational levels, and the transitions between them, depends critically upon the type of electronic state involved. Consequently we will be deeply concerned with the many different types of electronic state which arise for diatomic molecules, and the molecular interactions which determine the nature and structure of the rotational levels. We will not, in general, be concerned with transitions between different electronic states, except for the double resonance studies described in the final chapter. The vibrational states of diatomic molecules are, in a sense, relatively uninteresting.

The detailed rotational structure and sub-structure does not usually depend upon the vibrational quantum number, except for the magnitudes of the molecular parameters. Furthermore, we will not be concerned with transitions between different vibrational levels.

Rotational level spacings, and hence the frequencies of transitions between rotational levels, depend upon the values of the rotational constant, B_v, and the rotational quantum number J, according to equation (1.25). The largest known rotational constant, for the lightest molecule (H_2), is about 60 cm^{-1}, so that rotational transitions in this and similar molecules will occur in the far-infrared region of the spectrum. As the molecular mass increases, rotational transition frequencies decrease, and rotational spectroscopy for most molecules occurs in the millimetre wave and microwave regions of the electromagnetic spectrum.

The fine and hyperfine splittings within a rotational level, and the transition frequencies between components, depend largely on whether the molecular species has a closed or open shell electronic structure. We will discuss these matters in more detail in section 1.6. For a closed shell molecule, that is, one in a $^1\Sigma^+$ state, intramolecular interactions are in general very small. They depend almost entirely on the presence of nuclei with spin magnetic moments, or with electric quadrupole moments. If both nuclei in a diatomic molecule have spin magnetic moments, there will be a magnetic interaction between them which leads to splitting of a rotational level. The interaction may occur as a through-space dipolar interaction, or it may arise through an isotropic scalar coupling brought about by the electrons. Dipolar interactions are much larger than the scalar spin–spin couplings, but even so only produce splittings of a few kHz in the most favourable cases. A molecule also possesses a magnetic moment by virtue of its rotational motion, which can interact with any nuclear spin magnetic moments present in the molecule. Nuclear and rotational magnetic moments interact with an applied magnetic field, and these interactions are at the heart of the molecular beam magnetic resonance studies described in chapter 8. The pioneering experiments in this field were carried out in the period 1935 to 1955; they are capable of exceptionally high spectroscopic resolution, with line widths sometimes only a fraction of a kHz, and they form the foundations of what came to be known as nuclear magnetic resonance [3]. Nuclear electric quadrupole moments, where present, interact with the electric field gradient caused by the other charges (nuclei and electrons) in a molecule and the resulting interaction, called the nuclear electric quadrupole interaction, can in certain cases be quite large (i.e. several GHz). This interaction may be studied through molecular beam magnetic resonance experiments, but it can also be important in conventional microwave absorption studies, as we describe in chapter 10. Magnetic resonance studies require the presence of a magnetic moment, but in the closely related technique of molecular beam electric resonance, the interaction between a molecular electric dipole moment and an applied electric field is used. These experiments are also described in detail in chapter 8. The magnetic resonance studies of closed shell molecules almost always involve transitions between components of a rotational level, and usually occur in the radiofrequency region of the spectrum. Electric resonance experiments, on the other hand, often deal with electric dipole transitions between rotational levels, and occur in the millimetre wave and microwave regions of the spectrum. Molecular beam electric resonance experiments are closely related to conventional absorption experiments.

Molecules with open shell electronic states, which are often highly reactive transient species called free radicals, introduce a range of new intramolecular interactions. The largest of these, which occurs in molecules with both spin and orbital angular momentum, is spin–orbit coupling. Spin–orbit interactions range from a few cm^{-1} to several thousand cm^{-1} and determine the overall pattern of the rotational levels and their associated spectroscopy. Molecules in $^2\Pi$ states are particularly important and will appear frequently in this book; the OH and CH radicals, in particular, are principal players who will make many appearances. If orbital angular momentum is not present, spin–orbit coupling is less important (though not completely absent). However, the magnetic moment due to electron spin is large and will interact with nuclear spin magnetic moments, to give nuclear hyperfine structure, and also with the rotational magnetic moment, giving rise to the so-called spin–rotation interaction. As important, however, is the strong interaction which occurs with an applied magnetic field. This interaction leads to magnetic resonance studies with bulk samples, performed at frequencies in the microwave region, or even in the far-infrared. The Zeeman interaction is used to tune spectroscopic transitions into resonance with fixed-frequency radiation; these experiments are described in detail in chapter 9. For various reasons they are capable of exceptionally high sensitivity, and consequently have been extremely important in the study of short-lived free radicals. It is, perhaps, important at this point to appreciate the difference between the molecular beam magnetic resonance experiments described in chapter 8, and the bulk studies described in chapter 9. In most of the molecular beam experiments the Zeeman interactions are used to control the molecular trajectories through the apparatus, and to produce state selectivity. Spectroscopic transitions, which may or may not involve Zeeman components, are detected through their effects on detected beam intensities. No attempt is made to detect the absorption or emission of electromagnetic radiation directly. Conversely, in the bulk magnetic resonance experiments, direct detection of the radiation is involved and the Zeeman effect is used to tune spectroscopic transitions into resonance with the radiation. Later in this chapter we will give a little more detail about electron spin and hyperfine interactions, as well as the Zeeman effect in open shell systems.

The final, but very important, point to be made in this section is that all of the experiments described and discussed in this book involve molecules in the gas phase. Moreover the gas pressures involved are sufficiently low that the molecular rotational motion is conserved. Just as importantly, quantised electronic orbital motion is not quenched by molecular collisions, as it would be at higher pressures. Of course, condensed phase studies are important in their own right, but they are different in a number of fundamental ways. In condensed phases rotational motion and electronic orbital angular momentum are both quenched. Anisotropic interactions, such as the dipolar interactions involving electron or nuclear spins, or both, can be studied in regularly oriented solids like single crystals, but are averaged in randomly oriented solids, like glasses. In isotropic liquids they drive time-dependent relaxation processes through a combination of the anisotropy and the tumbling Brownian motion of the molecules. It should also be remembered that the strong *intermolecular* interactions that occur in solids can substantially change the magnitudes of the *intramolecular* interactions, like hyperfine interactions.

1.5. Historical perspectives

A major reference point in the history of diatomic molecule spectroscopy was the publication of a classic book by Herzberg in 1950 [4]; this book was, in fact, an extensively revised and enlarged version of one published earlier in 1939. Herzberg's book was entitled *Spectra of Diatomic Molecules*, and it deals almost entirely with electronic spectroscopy. In the years leading up to and beyond 1950, spectrographic techniques using photographic plates were almost universally employed. They covered a wide wavelength range, from the far-ultraviolet to the near-infrared, and at their best presented a comprehensive view of the complete rovibronic band system of one or more electronic transitions. In Herzberg's hands these techniques were indeed presented at their best, and his book gives masterly descriptions of the methods used to obtain and analyse these beautiful spectra. For both diatomic and polyatomic molecules, most of what we now know and understand about molecular shapes, geometry, structure, dynamics, and electronic structure, has come from spectrographic studies of the type described by Herzberg. One could not improve on his exposition of the rules leading to our comprehension of these spectra, and there is no need to attempt to do so. It is, however, a rather sad fact that the classic spectrographic techniques seem now to be regarded as obsolete; most of the magnificent instruments which were used have been scrapped. The main thrust now is to use lasers to probe intimate details with much greater sensitivity, specificity and resolution, but such studies would not be possible without the foundations provided by the classic techniques. Perhaps one day they will, of necessity, return.

Almost all of the spectroscopy described in our book involves techniques which have been developed since the publication of Herzberg's book. Rotational energy levels were very well understood in 1950, and the analysis of rotational structure in electronic spectra was a major part of the subject. The major disadvantage of the experimental methods used was, however, the fact that the resolution was limited by Doppler broadening. The Doppler line width depends upon the spectroscopic wavelength, the molecular mass, the effective translational temperature, and other factors. However, a ballpark figure for the Doppler line width of 0.1 cm^{-1} would not be far out in most cases. Concealed within that 0.1 cm^{-1} are many subtle and fascinating details of molecular structure which are major parts of the subject of this book.

In 1950, microwave and molecular beam methods were just beginning to be developed, and they are mentioned briefly by Herzberg in his book. Microwave spectroscopy was given a boost by war-time research on radar, with the development of suitable radiation sources and transmission components; an early review of the subject was given by Gordy [5], one of its pioneers. Cooley and Rohrbaugh [6] observed the first three rotational transitions of HI in 1945, whilst Weidner [7] and Townes, Merritt and Wright [8] observed microwave transitions of the ICl molecule. Because of the much reduced Doppler width at the long wavelengths in the microwave region, nuclear hyperfine effects were observed. Such effects were already known in atomic spectroscopy, but not in molecular electronic spectra apart from some observations on HgH. Microwave transitions in the O_2 molecule were observed by Beringer [9] in 1946, and Beringer and Castle [10] in 1949 observed transitions between the Zeeman components of the rotational levels in O_2 and NO, the first examples of magnetic resonance in open shell molecules. Chapter 9 in this book is devoted to the now large and important subject of magnetic resonance spectroscopy in bulk gaseous samples.

The molecular beam radiofrequency magnetic resonance spectrum of H_2 was first observed by Kellogg, Rabi, Ramsey and Zacharias [11] in 1939, and was further developed in the post-war years. An analogous radiofrequency electric resonance spectrum of CsF was described by Hughes [12] in 1947, and again the technique underwent extensive development in the next thirty years. These molecular beam experiments, which had important precursors in atomic beam spectroscopy, are very different from the traditional spectroscopic experiments described by Herzberg in his book. They are capable of very high spectroscopic resolution, partly because they usually involve radio- or microwave frequencies, partly because of the absence of collisional effects, and partly because residual Doppler effects can be removed by appropriate relative spatial alignment of the molecular beam and the electromagnetic radiation. All of these matters are discussed in great detail in chapter 8. Finally in this brief review of the techniques that were developed after Herzberg's book, we should mention the laser, which now dominates electronic spectroscopy, and much of vibrational spectroscopy as well. Laser spectroscopy as such is not an important part of this book, apart from far-infrared magnetic resonance studies, but the use of lasers, both visible and infrared, in double resonance experiments is an important aspect of chapter 11. Lasers have made it possible to apply the techniques of radiofrequency and microwave spectroscopy to excited electronic states, an aspect of the subject which is likely to be developed much further.

Herzberg's book was therefore perfectly timed. The electronic spectroscopy of diatomic molecules was well developed and understood, and continues to be important [13]. Hopefully our book is also well timed; the molecular beam magnetic and electric resonance experiments are becoming less common, and may now almost be regarded as classic techniques! Magnetic resonance experiments on bulk gaseous samples are likely to continue to be important in the study of free radicals, particularly because of their very high sensitivity. Double resonance is important, in the study of excited states, but also in the route it provides towards the study of much heavier molecules where sensitivity considerations become increasingly important. Finally, pure rotational spectroscopy has assumed even greater importance because of its relationship with radioastronomy and the study of interstellar molecules, and because of its applications in the study of atmospheric chemistry.

1.6. Fine structure and hyperfine structure of rotational levels

1.6.1. Introduction

We outlined in section 1.4 the coordinate transformations which enable us to separate the rotational motion of a diatomic molecule from the electronic and vibrational motions. We pointed out that the spectroscopy described in this book involves either transitions *between* different rotational levels, or transitions between the various subcomponents *within* a single rotational level; additional effects arising from applied electric or magnetic fields may or may not be present. We now outline very briefly the origin and nature of the sub-structure which is possible for a single rotational level in different electronic states. All of the topics mentioned in this section will be developed in considerable depth elsewhere in the book, but we hope that an elementary introduction will be useful, especially for the reader approaching the subject for the first time. As we will see, the detailed sub-structure of a rotational level depends upon the nature of the electronic state being considered. We can divide the electronic states into three different types, namely, closed shell states without electronic angular momentum, open shell states with electron spin angular momentum, and open shell states with both orbital and spin angular momentum. There is also a small number of cases where an electronic state has orbital but not spin angular momentum.

We will present the *effective* Hamiltonian terms which describe the interactions considered, sometimes using cartesian methods but mainly using spherical tensor methods for describing the components. These subjects are discussed extensively in chapters 5 and 7, and at this stage we merely quote important results without justification. We will use the symbol T to denote a spherical tensor, with the particular operator involved shown in brackets. The *rank* of the tensor is indicated as a post-superscript, and the *component* as a post-subscript. For example, the electron spin vector $\boldsymbol{S}$ is a first-rank tensor, $\mathrm{T}^1(\boldsymbol{S})$, and its three spherical components are related to cartesian components in the following way:

$$\begin{aligned}\mathrm{T}^1_0(\boldsymbol{S}) &= S_z,\\ \mathrm{T}^1_1(\boldsymbol{S}) &= -(1/\sqrt{2})(S_x + \mathrm{i}S_y),\\ \mathrm{T}^1_{-1}(\boldsymbol{S}) &= (1/\sqrt{2})(S_x - \mathrm{i}S_y).\end{aligned} \tag{1.26}$$

The components may be expressed in either a space-fixed axis system (p) or a molecule-fixed system (q). The early literature used cartesian coordinate systems, but for the past fifty years spherical tensors have become increasingly common. They have many advantages, chief of which is that they make maximum use of molecular symmetry. As we shall see, the rotational eigenfunctions are essentially spherical harmonics; we will also find that transformations between space- and molecule-fixed axes systems, which arise when external fields are involved, are very much simpler using rotation matrices rather than direction cosines involving cartesian components.

1.6.2. $^1\Sigma^+$ states

In a diatomic, or linear polyatomic molecule, the energies of the rotational levels within a vibrational level v are given by

$$E(v, J) = B_v J(J+1) - D_v J^2(J+1)^2 + H_v J^3(J+1)^3 + \cdots, \qquad (1.27)$$

where the rotational quantum number, J, takes integral values 0, 1, 2, etc. Provided the molecule is heteronuclear, with an electric dipole moment, rotational transitions between adjacent rotational levels ($\Delta J = \pm 1$) are electric-dipole allowed. The extent of the spectrum depends upon how many rotational levels are populated in the gaseous sample, which is determined by the Boltzman distribution law for a system in thermal equilibrium. The rotational transition frequencies increase as J increases, as (1.27) shows.

Any additional complications depend entirely on the nature of the nuclei involved. General Appendix B presents a list of the naturally occurring isotopes, with their spins, magnetic moments and electric quadrupole moments. Magnetic and electric interactions involving these moments can and will occur, the most important in a $^1\Sigma$ state being the electric quadrupole interaction between the nuclear quadrupole moment and an electric field gradient at the nucleus. Nuclei possessing a quadrupole moment must also have a spin $\boldsymbol{I}$ equal to 1 or more, and the extent of the quadrupole splitting of a rotational level depends upon the value of the nuclear spin. One of the most important quadrupolar nuclei is the deuteron, and quadrupole effects were probably first observed and analysed in the molecular beam magnetic resonance spectra of HD and D_2. In describing the energy levels we will often use a hyperfine-coupled representation, written as a ket $|\eta, J, I, F\rangle$, where the symbol η represents all other quantum numbers not specified, particularly those describing the electronic and vibrational state. For any given rotational level J, the total angular momentum F takes all values $J + I, J + I - 1, \ldots, |J - I|$, so that there can be splitting into a maximum of $2I + 1$ hyperfine levels for a single quadrupolar nucleus provided $J \geq I$. Such a case is shown schematically in figure 1.4 for the AlF molecule [14]; the ^{27}Al nucleus has a spin I of 5/2 and a large quadrupole moment. The $J = 0$ rotational level has no quadrupole splitting but $J = 1$ is split into three components as shown. An electric dipole $J = 1 \leftarrow 0$ rotational transition between adjacent rotational levels will exhibit a quadrupole splitting, as indicated. Alternatively, a spectrum arising from transitions within a single rotational level is possible, as indicated for CsF in figure 1.5. In this case [12] the ^{133}Cs nucleus has a spin of 7/2, and there is also an additional doublet splitting from the ^{19}F nucleus, arising from its magnetic dipole moment, which we will discuss shortly. There are other subtle aspects of this spectrum, one of them being that if the spectrum is recorded in the presence of a weak electric field, the transitions shown, which would be expected to have magnetic dipole intensity only, acquire electric dipole intensity. The full details are given in chapter 8.

The essential features of the electric quadrupole interaction can, hopefully, be appreciated with the aid of figure 1.6. The Z direction defines the direction of the

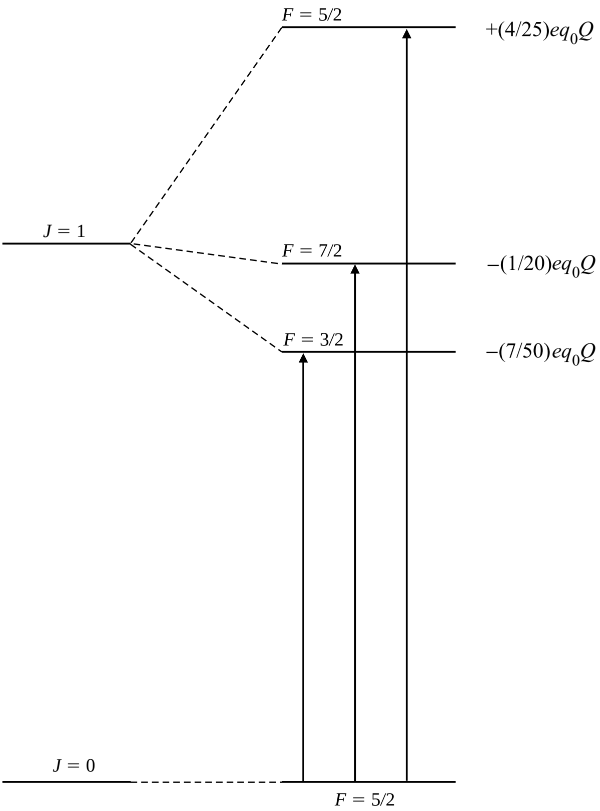

Figure 1.4. Splitting of the $J = 1$ rotational level of ^{27}Al^{19}F arising from the ^{27}Al quadrupole interaction with spin $I = 5/2$, and the resulting hyperfine splitting of the rotational transition. The magnetic interactions involving the ^{19}F nucleus are too small to be observed in this case.

electric field gradient, produced mainly by the electrons in the molecule. The total charge distribution of the nucleus may be decomposed into the sum of monopole, quadrupole, hexadecapole moments; the quadrupole distribution may be represented as a cigar-shaped distribution of charge having cylindrical symmetry about a principal axis fixed in the nucleus, which we define as the nuclear z axis. The quadrupolar charge distribution may be appreciated by considering the nuclear charge distribution at symmetrically disposed points on the $+z, -z, +x, -x$ axes. As we see from figure 1.6. the nuclear charge is $\delta-$ at the $\pm x$ points and $\delta+$ at the $\pm z$ points.

For a nucleus of spin $I = 1$ there are three allowed spatial orientations of the spin; in figure 1.6 these three orientations may be identified with those in which the nuclear z axis is coincident with Z, perpendicular to Z, and antiparallel to Z. These three orientations correspond to projection quantum numbers $M_I = +1$, 0 and -1 respectively, and it is clear from the figure that the state with $M_I = 0$ has a different electrostatic energy from the states with $M_I = \pm 1$. This 'quadrupole splitting' depends upon the sizes of the nuclear quadrupole moment and the electric field gradient.

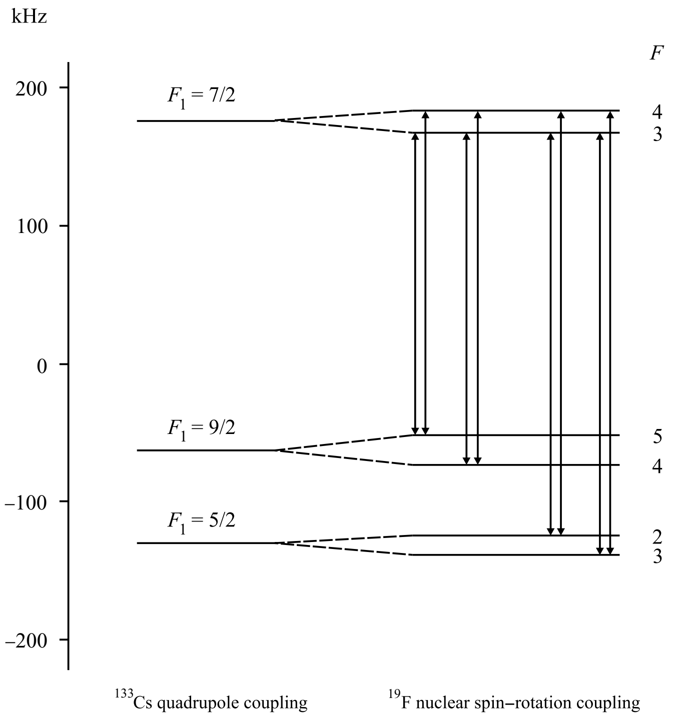
kHz
F
200
100
0
−100
−200
F_1 = 7/2
F_1 = 9/2
F_1 = 5/2
4
3
5
4
2
3
^{133}Cs quadrupole coupling
^{19}F nuclear spin–rotation coupling

Figure 1.5. Nuclear hyperfine splitting of the $J = 1$ rotational level of CsF. The major splitting is the result of the ^{133}Cs quadrupole interaction, and the smaller doublet splitting is caused by the ^{19}F interaction (see text).

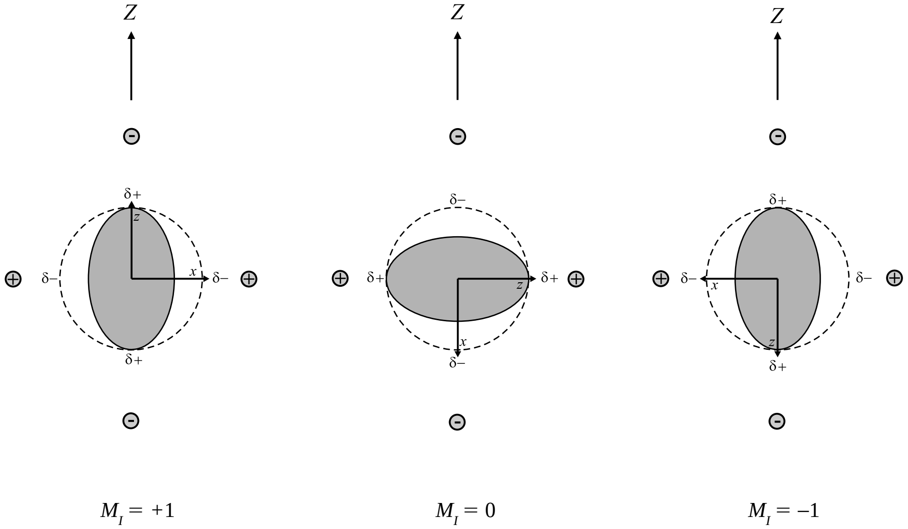
Z
Z
Z
δ+
z
δ−
x
δ−
δ+
δ−
δ+
z
δ+
x
δ−
δ+
δ−
x
δ−
z
δ+
$M_I = +1$
$M_I = 0$
$M_I = -1$

Figure 1.6. Orientation of a nucleus ($I = 1$) with an electric quadrupole moment in an electric field gradient.

We show elsewhere in this book that the quadrupole interaction may be represented as the scalar product of two second-rank spherical tensors,

$$\mathcal{H}_{\mathrm{Q}} = -e\mathrm{T}^2(\nabla \boldsymbol{E}) \cdot \mathrm{T}^2(\boldsymbol{Q}), \tag{1.28}$$

where the details of the electric field gradient are contained within the first tensor in (1.28) and the nuclear quadrupole moment is contained within the second tensor. We show elsewhere (chapter 8, for example) that the diagonal quadrupole energy obtained from (1.28) is given by

$$E_{\mathbf{Q}} = -\frac{eq_0 Q}{2I(2I-1)(2J-1)(2J+3)}\{(3/4)C(C+1) - I(I+1)J(J+1)\}, \tag{1.29}$$

where $C = F(F+1) - I(I+1) - F(F+1)$. The quantity $eq_0 Q$ in (1.29) is called the quadrupole coupling constant, q_0 being the electric field gradient (actually its negative) and eQ the quadrupole moment of the ^{133}Cs nucleus. The value of $eq_0 Q$ for ^{133}Cs in CsF is 1.237 MHz.

The quadrupole coupling is very much the most important nuclear hyperfine interaction in $^1\Sigma^+$ states, and it takes the same form in open shell states as in closed shells. We turn now to the much smaller interactions involving magnetic dipole moments, two types of which may be present. A nuclear spin $\boldsymbol{I}$ gives rise to a magnetic moment $\boldsymbol{\mu}_I$,

$$\boldsymbol{\mu}_I = g_N \mu_N \boldsymbol{I}, \tag{1.30}$$

where g_N is the g-factor for the particular nucleus in question and μ_N is the nuclear magneton. In addition, the rotation of the nuclei and electrons gives rise to a rotational magnetic moment, whose value depends upon the rotational quantum number,

$$\boldsymbol{\mu}_J = \mu_N \boldsymbol{J}. \tag{1.31}$$

The magnetic moments given above will interact with an applied magnetic field, and these interactions are discussed extensively in chapter 8. In some diatomic molecules both nuclei have non-zero spin and an associated magnetic moment. The magnetic interactions which then occur are the nuclear spin–rotation interactions, represented by the operator

$$\mathcal{H}_{\mathrm{nsr}} = \sum_{\alpha=1,2} c_\alpha \mathrm{T}^1(\boldsymbol{J}) \cdot \mathrm{T}^1(\boldsymbol{I}_\alpha), \tag{1.32}$$

and the nuclear spin–spin interactions. Here two different interactions are possible. The largest and most important is the through-space dipolar interaction, which in its classical form is represented by the operator

$$\mathcal{H}_{\mathrm{dip}} = g_1 g_2 \mu_N^2 (\mu_0/4\pi)\left\{\frac{\boldsymbol{I}_1 \cdot \boldsymbol{I}_2}{R^3} - \frac{3(\boldsymbol{I}_1 \cdot \boldsymbol{R})(\boldsymbol{I}_2 \cdot \boldsymbol{R})}{R^5}\right\}. \tag{1.33}$$

Here $\boldsymbol{I}_1, \boldsymbol{I}_2$ and g_1, g_2 are the spins and g-factors of nuclei 1 and 2 and R is the distance between them. In spherical tensor form the interaction may be written

$$\mathcal{H}_{\mathrm{dip}} = -g_1 g_2 \mu_N^2 (\mu_0/4\pi)\sqrt{6}\mathrm{T}^2(\boldsymbol{C}) \cdot \mathrm{T}^2(\boldsymbol{I}_1, \boldsymbol{I}_2), \tag{1.34}$$

where the second-rank tensors are defined as follows:

$$\mathrm{T}^2_p(\boldsymbol{I}_1, \boldsymbol{I}_2) = (-1)^p\sqrt{5}\sum_{p_1,p_2}\begin{pmatrix} 1 & 1 & 2 \\ p_1 & p_2 & -p \end{pmatrix}\mathrm{T}^1_{p_1}(\boldsymbol{I}_1)\mathrm{T}^1_{p_2}(\boldsymbol{I}_2), \tag{1.35}$$

$$\mathrm{T}^2_q(\boldsymbol{C}) = \langle C^2_q(\theta, \phi)R^{-3}\rangle. \tag{1.36}$$

These expressions require some detailed explanation, and the reader might wish to advance to chapter 5 at this point. First, here and elsewhere, the subscripts p and q refer to space-fixed and molecule-fixed axes respectively. Equation (1.35) which describes the construction of a second-rank tensor from two first-rank tensors contains a vector coupling coefficient called a Wigner 3-j symbol. Equation (1.36) contains a spherical harmonic function which gives the necessary geometric information. The equivalence of (1.34) and (1.33) is demonstrated in appendix 8.1, which also introduces another spherical tensor form for the dipolar interaction. The most important feature is, of course, the R^{-3} dependence of the interaction. In the H_2 molecule the proton–proton dipolar coupling is about 60 kHz, which is readily determinable in the high-resolution molecular beam magnetic resonance studies.

The second interaction between two nuclear spins in a diatomic molecule is a scalar coupling,

$$\mathcal{H}_{\mathrm{scalar}} = c_{\mathrm{s}}\mathrm{T}^1(\boldsymbol{I}_1)\cdot\mathrm{T}^1(\boldsymbol{I}_2), \tag{1.37}$$

which is often described as the electron-coupled spin–spin interaction because the mechanism involves the transmission of nuclear spin orientation through the intervening electrons (see section 1.7). This coupling is very small compared with the dipolar interaction, and is usually negligible in gas phase studies. It is, however, extremely important in liquid phase nuclear magnetic resonance because, unlike the dipolar coupling, it is not averaged to zero by the tumbling motion of the molecules.

The remaining important type of magnetic interaction is that between the rotational magnetic moment and any nuclear spin magnetic moments, given in equation (1.32). In the case of H_2 the constant c has the value 113.9 kHz. The doublet splitting in the spectrum of CsF, shown in figure 1.5, is due to the ^{19}F nuclear spin–rotation interaction. Note also that in this case the hyperfine basis kets take the form $|\eta, J, I_1, F_1; I_2, F\rangle$ where I_1 is the spin of ^{133}Cs (value 7/2) and I_2 is the spin of ^{19}F value 1/2. Hence for $J = 1$, F_1 can take the values 9/2, 7/2 and 5/2 as shown, and F takes values $F_1 \pm 1/2$. Other possible magnetic interactions in CsF are too small to be observed.

The remaining important magnetic interactions to be considered are those which arise when a static magnetic field $\boldsymbol{B}$ is applied. The Zeeman interaction with a nuclear spin magnetic moment is represented by the Hamiltonian term

$$\mathcal{H}_{\mathrm{Z}} = -\sum_{\alpha=1,2} g^{\alpha}_N\mu_N\mathrm{T}^1(\boldsymbol{B})\cdot\mathrm{T}^1(\boldsymbol{I}_\alpha), \tag{1.38}$$

and since the direction of the magnetic field is usually taken to define the space-fixed

Z or $p = 0$ direction, the scalar product in (1.38) contracts to

$$\mathcal{H}_{\mathrm{Z}} = -\sum_{\alpha=1,2} g_N^{\alpha} \mu_N \mathrm{T}_0^1(\boldsymbol{B}) \mathrm{T}_0^1(\boldsymbol{I}_{\alpha}). \tag{1.39}$$

The nuclear spin Zeeman levels then have energies given by

$$E_{\mathrm{Z}} = -\sum_{\alpha=1,2} g_N^{\alpha} \mu_N B_Z M_{I_{\alpha}}, \tag{1.40}$$

where the projection quantum number M_I takes the $2I + 1$ values from $-I$ to $+I$. The nuclear spin Zeeman interaction in discussed extensively in chapter 8. In molecular beam experiments it is used for magnetic state selection, and the radiofrequency transitions studied are usually those with the selection rule $\Delta M_I = \pm 1$ observed in the presence of an applied magnetic field. We will also see, in chapter 8, that the simple expression (1.38) is modified by the inclusion of a screening factor,

$$\mathcal{H}_{\mathrm{Z}} = -\sum_{\alpha=1,2} g_N^{\alpha} \mu_N \mathrm{T}^1(\boldsymbol{B}) \cdot \mathrm{T}^1(\boldsymbol{I}_{\alpha}) \{1 - \sigma_{\alpha}(\boldsymbol{J})\}, \tag{1.41}$$

arising mainly because of the diamagnetic circulation of the electrons in the presence of the magnetic field. In liquid phase nuclear magnetic resonance this screening gives rise to what is known as the ‘chemical shift’.

The rotational magnetic moment also interacts with an applied magnetic field, the interaction term being very similar to (1.41) above, i.e.

$$\mathcal{H}_{JZ} = -g_r \mu_N \mathrm{T}^1(\boldsymbol{B}) \cdot \mathrm{T}^1(\boldsymbol{J}) \{1 - \sigma(\boldsymbol{J})\}, \tag{1.42}$$

where g_r is the rotational g-factor. In a molecule where there are no nuclear spins present, the rotational Zeeman interaction can be used for selection of M_J states.

Finally in this section on ${}^1\Sigma^+$ states we must include the Stark interaction which occurs when an electric field ($\boldsymbol{E}$) is applied to a molecule possessing a permanent electric dipole moment ($\boldsymbol{\mu}_e$):

$$\mathcal{H}_{\mathrm{E}} = -\mathrm{T}^1(\boldsymbol{\mu}_e) \cdot \mathrm{T}^1(\boldsymbol{E}). \tag{1.43}$$

As with the Zeeman interaction discussed earlier, (1.43) is usually contracted to the space-fixed $p = 0$ component. An extremely important difference, however, is that in contrast to the nuclear spin Zeeman effect, the Stark effect in a ${}^1\Sigma$ state is second-order, which means that the electric field *mixes* different rotational levels. This aspect is thoroughly discussed in the second half of chapter 8; the second-order Stark effect is the engine of molecular beam electric resonance studies, and the spectra, such as that of CsF discussed earlier, are usually recorded in the presence of an applied electric field.

Whilst the most important examples of Zeeman and Stark effects in ${}^1\Sigma$ states are found in molecular beam studies, they can also be important in conventional absorption microwave rotational spectroscopy, as we describe in chapter 10. The use of the Stark effect to determine molecular dipole moments is a very important example.

1.6.3. Open shell Σ states

We now proceed to consider the magnetic interactions involving the electron spin $\boldsymbol{S}$ in Σ states with open shell electronic structures. The magnetic dipole moment arising from electron spin is

$$\boldsymbol{\mu}_S = -g_S \mu_B \boldsymbol{S}, \tag{1.44}$$

where g_S is the free electron g-factor, with the value 2.0023, and μ_B is the electron Bohr magneton; μ_B is almost two thousand times larger than the nuclear magneton, μ_N, so we see at once that magnetic interactions from electron spin are very much larger than those involving nuclear spin, considered in the previous sub-section.

With the introduction of electronic angular momentum, we have to consider how the spin might be coupled to the rotational motion of the molecule. This question becomes even more important when electronic orbital angular momentum is involved. The various coupling schemes give rise to what are known as Hund's coupling cases; they are discussed in detail in chapter 6, and many practical examples will be encountered elsewhere in this book. If only electron spin is involved, the important question is whether it is quantised in a space-fixed axis system, or molecule-fixed. In this section we confine ourselves to space quantisation, which corresponds to Hund's case (b).

We deal first with molecules containing one unpaired electron ($S = 1/2$) where magnetic nuclei are not present. The electron spin magnetic moment then interacts with the magnetic moment due to molecular rotation, the interaction being represented by the Hamiltonian term

$$\mathcal{H}_{\rm sr} = \gamma \mathrm{T}^1(\boldsymbol{S}) \cdot \mathrm{T}^1(\boldsymbol{N}), \tag{1.45}$$

in which γ is the spin–rotation coupling constant. As was originally shown by Hund [15] and Van Vleck [16], each rotational level in a given vibrational level (v) of a $^2\Sigma$ state is split into a spin doublet, with energies

$$\begin{aligned} F_1(N) &= B_v N(N+1) + (1/2)\gamma_v N, \\ F_2(N) &= B_v N(N+1) - (1/2)\gamma_v (N+1). \end{aligned} \tag{1.46}$$

The F_1 levels correspond to $J = N + 1/2$ and the F_2 levels to $J = N - 1/2$. A typical rotational energy level diagram is shown in figure 1.7(a); each rotational transition ($\Delta N = \pm 1$) is split into a doublet (with $\Delta J = \pm 1$) and a weaker satellite ($\Delta J = 0$). This seems a simple conclusion, except that Van Vleck [16] showed that the spin splitting of each rotation level is only partly the result of the rotational magnetic moment in the direction of $\boldsymbol{N}$. The other part comes from electronic orbital angular momentum in the Σ state which precesses at right angles about the internuclear axis; in other words, although the expectation value of $\boldsymbol{L}$ is zero in a pure Σ state, the spin–orbit coupling operator mixes the Σ state with excited Π states. This introduces an additional non-zero magnetic moment in the direction of $\boldsymbol{N}$, which contributes to the spin–rotation coupling. We will return to this important subject in the next section; it represents

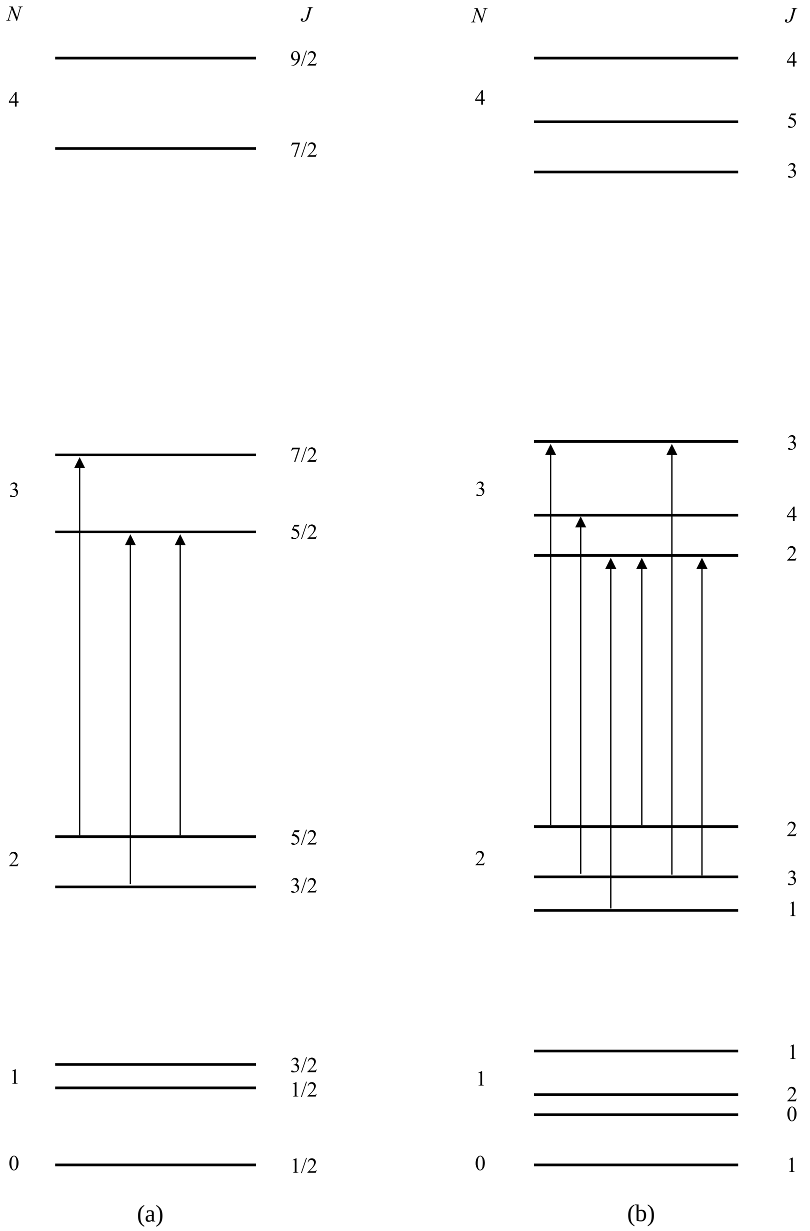

(a) (b)

Figure 1.7. (a) Lower rotational levels and transitions in a case (b) $^2\Sigma$ state, showing the spin splitting of a rotational transition. (b) Lower rotational levels and transitions in a case (b) $^3\Sigma$ state, showing the spin splitting of a rotational transition.

our first encounter with the very important concept of the *effective* Hamiltonian. What looks like a spin–rotation interaction is not entirely what it seems!

The lower rotational levels for a case (b) $^3\Sigma$ state are shown in figure 1.7(b). The spin–rotation interaction takes the same form as for a $^2\Sigma$ state, given in equation (1.45), but in addition there is an important interaction between the spins of the two unpaired electrons, called the electron spin–spin interaction; this is usually larger than the spin–rotation interaction. The spin–spin interaction can be represented in a number of different ways, depending upon the molecule under investigation. Initially we might regard the interaction as being analogous to the classical interaction between two magnetic dipole moments so that, following equation (1.33) for nuclear spins, we write the interaction as

$$\mathcal{H}_{ss} = g_S^2\mu_B^2(\mu_0/4\pi)\left\{\frac{\boldsymbol{S}_1\cdot\boldsymbol{S}_2}{r^3} - \frac{3(\boldsymbol{S}_1\cdot\boldsymbol{r})(\boldsymbol{S}_2\cdot\boldsymbol{r})}{r^5}\right\}, \qquad (1.47)$$

where $\boldsymbol{S}_1$ and $\boldsymbol{S}_2$ are the spins of the individual electrons, and r is the distance between them. Of course, the electrons are not point charges, so that r is an average distance which can be calculated from a suitable electronic wave function. Again, by analogy with our previous treatment of nuclear spins, the electron spin dipolar interaction can be represented in spherical tensor form by the operator

$$\mathcal{H}_{ss} = -g_S^2\mu_B^2(\mu_0/4\pi)\sqrt{6}\mathrm{T}^2(\boldsymbol{C})\cdot\mathrm{T}^2(\boldsymbol{S}_1,\boldsymbol{S}_2), \qquad (1.48)$$

where, as before, $\mathrm{T}^2(\boldsymbol{C})$ represents the spherical harmonic functions, the $q=0$ component being given by

$$\mathrm{T}_0^2(\boldsymbol{C}) = C_0^2(\theta,\phi)\langle r^{-3}\rangle = \left(\frac{4\pi}{5}\right)^{1/2} Y_{2,0}(\theta,\phi)\langle r^{-3}\rangle = \frac{1}{2}\langle(2z^2-x^2-y^2)\rangle\langle r^{-5}\rangle. \qquad (1.49)$$

In appendix 8.3 we show that (1.48) with $q=0$ leads to the simple expression,

$$\mathcal{H}_{ss} = \frac{2}{3}\lambda\left(3S_z^2 - \boldsymbol{S}^2\right), \qquad (1.50)$$

where z is the internuclear axis and λ is called the spin–spin coupling constant. Provided λ is not too large compared with the rotational constant, Kramers [17] showed that each rotational level is split into a spin triplet, with relative component energies

$$\begin{aligned} F_1(N) &= B_v N(N+1) - \frac{2\lambda(N+1)}{(2N+3)} + \gamma_v(N+1),\\ F_2(N) &= B_v N(N+1), \\ F_3(N) &= B_v N(N+1) - \frac{2\lambda N}{(2N-1)} - \gamma_v N. \end{aligned} \qquad (1.51)$$

where F_1, F_2, F_3 refer to levels with $J = N+1$, N and $N-1$. More accurate formulae were given by Schlapp [18] and, neglecting the small vibrational dependence of λ and γ, these are

$$\begin{aligned} F_1(N) &= B_v N(N+1) + (2N+3)B_v - \lambda - \left\{(2N+3)^2B_v^2 + \lambda^2 - 2\lambda B_v\right\}^{1/2} + \gamma_v(N+1),\\ F_2(N) &= B_v N(N+1), \\ F_3(N) &= B_v N(N+1) - (2N-1)B_v - \lambda + \left\{(2N-1)^2B_v^2 + \lambda^2 - 2\lambda B_v\right\}^{1/2} - \gamma_v N. \end{aligned} \qquad (1.52)$$

The molecule O_2 in its ${}^3\Sigma_g^-$ ground state is a good example of a case (b) molecule, and the triplet energies agree with (1.52), the values of the constants being $B_0 = 1.437\,77\ \mathrm{cm}^{-1}$, $\lambda = 1.984\ \mathrm{cm}^{-1}$, $\gamma_0 = -0.0084\ \mathrm{cm}^{-1}$. Note that yet another spherical tensor form for the dipolar interaction which is sometimes used is

$$\mathcal{H}_{\mathrm{ss}} = 2\lambda \mathrm{T}^2(\boldsymbol{S}, \boldsymbol{S}) \cdot \mathrm{T}^2(\boldsymbol{n}, \boldsymbol{n}), \tag{1.53}$$

where $\boldsymbol{n}$ is a unit vector along the internuclear axis and $\boldsymbol{S}$ is the total spin of 1. Again, the relationship of this form to the others is described in appendix 8.3. A typical pattern of rotational levels for a $^3\Sigma$ state with the spin splitting is shown in figure 1.7(b), together with the allowed rotational transitions. Once again, spin–orbit coupling can mix a $^3\Sigma$ state with nearby Π states and contribute to the value of the constant λ. We show in chapter 9 that in the SeO molecule the spin–orbit coupling is so strong that the case (b) pattern of rotational levels no longer holds, and a case (a) coupling scheme is more appropriate. The formulae given above are then not applicable.

The remaining important interactions which can occur for a $^2\Sigma$ or $^3\Sigma$ molecule involve the presence of nuclear spin. Interactions between the electron spin and nuclear spin magnetic moments are called 'hyperfine' interactions, and there are two important ones. The first is called the Fermi contact interaction, and if both nuclei have non-zero spin, each interaction is represented by the Hamiltonian term

$$\mathcal{H}_{\mathrm{F}} = b_{\mathrm{F}} \mathrm{T}^1(\boldsymbol{S}) \cdot \mathrm{T}^1(\boldsymbol{I}). \tag{1.54}$$

The Fermi contact constant b_{F} is given by

$$b_{\mathrm{F}} = \left(\frac{2}{3}\right) g_S \mu_B g_N \mu_N \mu_0 \int \psi^2(\boldsymbol{r}) \delta(\boldsymbol{r})\, \mathrm{d}\boldsymbol{r}, \tag{1.55}$$

where the function $\delta(\boldsymbol{r})$, called the Dirac delta function, imposes the condition that $\boldsymbol{r} = 0$ when we integrate over the probability density of the wave function of the unpaired electron. Hence the contact interaction can only occur when the unpaired electron has a finite probability density at the nucleus, which means that the wave function must have some s-orbital character (i.e. $\psi(0)^2 \neq 0$).

The second important hyperfine interaction is the dipolar interaction and by analogy with equations (1.34) and (1.48) it may be expressed in spherical tensor form by the expression

$$\mathcal{H}_{\mathrm{dip}} = \sqrt{6} g_S \mu_B g_N \mu_N (\mu_0/4\pi) \mathrm{T}^2(\boldsymbol{C}) \cdot \mathrm{T}^2(\boldsymbol{S}, \boldsymbol{I}). \tag{1.56}$$

There are some situations when this is the most convenient representation of the dipolar coupling, for example, when $\boldsymbol{S}$ and $\boldsymbol{I}$ are very strongly coupled to each other but weakly coupled to the molecular rotation, as in the H_2^+ ion. However, an alternative form which is often more suitable is

$$\mathcal{H}_{\mathrm{dip}} = -\sqrt{10} g_S \mu_B g_N \mu_N (\mu_0/4\pi) \mathrm{T}^1(\boldsymbol{I}) \cdot \mathrm{T}^1(\boldsymbol{S}, \boldsymbol{C}^2). \tag{1.57}$$

The spherical components of the new first-rank tensor in (1.57) are defined, in the molecule-fixed axes system, by

$$\mathrm{T}^1_q(\boldsymbol{S}, \boldsymbol{C}^2) = \sqrt{3} \sum_{q_1, q_2} (-1)^q \mathrm{T}^1_{q_1}(\boldsymbol{S}) \mathrm{T}^2_{q_2}(\boldsymbol{C}) \begin{pmatrix} 1 & 2 & 1 \\ q_1 & q_2 & -q \end{pmatrix}, \tag{1.58}$$

where, as before,

$$\mathrm{T}^2_{q_2}(\boldsymbol{C}) = C^2_{q_2}(\theta, \phi)(r^{-3}). \tag{1.59}$$

The relationships between the various forms of the dipolar Hamiltonian are explained in appendix 8.2. As we see from (1.59), the dipolar interaction has various components in the molecule-fixed axis system but the most important one, and often the only one to be determined from experiment, is $\mathrm{T}^2_0(\boldsymbol{C})$. This leads us to define a constant t_0, the axial dipolar hyperfine component, given in SI units by,

$$t_0 = g_S \mu_B g_N \mu_N (\mu_0/4\pi)\mathrm{T}^2_0(\boldsymbol{C}) = \frac{1}{2} g_S \mu_B g_N \mu_N (\mu_0/4\pi)\left\langle \frac{(3\cos^2\theta - 1)}{r^3} \right\rangle. \tag{1.60}$$

The most important examples of $^2\Sigma$ states to be described in this book are CO$^+$, where there is no nuclear hyperfine coupling in the main isotopomer, CN, which has ^{14}N hyperfine interaction, and the H_2^+ ion. A number of different $^3\Sigma$ states are described, with and without hyperfine coupling. A particularly important and interesting example is N_2 in its $A\,^3\Sigma_u^+$ excited state, studied by De Santis, Lurio, Miller and Freund [19] using molecular beam magnetic resonance. The details are described in chapter 8; the only aspect to be mentioned here is that in a homonuclear molecule like N_2, the individual nuclear spins ($I = 1$ for ^{14}N) are coupled to form a total spin, I_T, which in this case takes the values 2, 1 and 0. The hyperfine Hamiltonian terms are then written in terms of the appropriate value of I_T. As we have already mentioned, the presence of one or more quadrupolar nuclei will give rise to electric quadrupole hyperfine interaction; the theory is essentially the same as that already presented for $^1\Sigma^+$ states.

Finally we note that the interaction with an applied magnetic field is important because of the large magnetic moment arising from the presence of electron spin (see (1.44)). The Zeeman interaction is represented by the Hamiltonian term

$$\mathcal{H}_Z = g_S \mu_B \mathrm{T}^1(\boldsymbol{B}) \cdot \mathrm{T}^1(\boldsymbol{S}) = g_S \mu_B B_{p=0} \mathrm{T}^1_{p=0}(\boldsymbol{S}) = g_S \mu_B B_Z \mathrm{T}^1_0(\boldsymbol{S}), \tag{1.61}$$

which, as we show, may again be contracted to a single $p = 0$ space-fixed component. As we will see, the Zeeman interaction is central to magnetic resonance studies, either with molecular beams as described in chapter 8 where radiofrequency spectroscopy is involved, or with bulk gases (chapter 9) where microwave or far-infrared radiation is employed. The magnetic resonance studies are, in general, of two kinds. For magnetic fields which are readily accessible in the laboratory, the Zeeman splitting of different M_S (or M_J) levels often corresponds to a microwave frequency. In many studies, therefore, the transitions studied obey a selection rule $\Delta M_S = \pm 1$ or $\Delta M_J = \pm 1$, and take place between levels which are otherwise degenerate in the absence of a magnetic field. There are, however, very important experiments where the transitions occur between levels which are already well separated in zero field; fixed frequency radiation is then used, with the transition energy mismatch being tuned to zero with an applied field. Far-infrared laser magnetic resonance studies are of this type. As we will see, the theoretical problem which must be solved concerns the competition between the Zeeman interaction, which tends to decouple the electron spin from the molecular framework, and intramolecular interactions like the electron spin dipolar coupling which tends to couple the spin orientation to the molecular orientation.

1.6.4. Open shell states with both spin and orbital angular momentum

Many free radicals in their electronic ground states, and also many excited electronic states of molecules with closed shell ground states, have electronic structures in which both electronic orbital and electronic spin angular momentum is present. The precession of electronic angular momentum, $\boldsymbol{L}$, around the internuclear axis in a diatomic molecule usually leads to defined components, Λ, along the axis, and states with $|\Lambda| = 0$, 1, 2, 3, etc., are called Σ, Π, Δ, Φ, etc., states. In most cases there is also spin angular momentum $\boldsymbol{S}$, and the electronic state is then labelled $^{2S+1}\Pi$, $^{2S+1}\Delta$, etc.

Questions arise immediately concerning the coupling of $\boldsymbol{L}$, $\boldsymbol{S}$ and the nuclear rotation, $\boldsymbol{R}$. The possible coupling cases, first outlined by Hund, are discussed in detail in chapter 6. Here we will adopt case (a), which is the one most commonly encountered in practice. The most important characteristic of case (a) is that Λ, the component of $\boldsymbol{L}$ along the internuclear axis, is indeed defined and we can use the labels Σ, Π, Δ, etc., as described above. The spin–orbit coupling can be represented in a simplified form by the Hamiltonian term

$$\mathcal{H}_{\rm SO} = A\mathrm{T}^1(\boldsymbol{L}) \cdot \mathrm{T}^1(\boldsymbol{S}) = A \sum_q (-1)^q \mathrm{T}^1_q(\boldsymbol{L})\mathrm{T}^1_{-q}(\boldsymbol{S}), \tag{1.62}$$

expanded in the molecule-fixed axis system as shown. The $q = 0$ term gives a diagonal energy $A\Lambda\Sigma$, where Σ is the component of the electron spin ($\boldsymbol{S}$) along the internuclear axis. The component of total electronic angular momentum along the internuclear axis is called Ω; it is given by $\Omega = \Lambda + \Sigma$.

If we are dealing with a $^2\Pi$ state, the possible values of the projection quantum numbers are as follows:

$$\begin{aligned} \Lambda &= +1, & \Sigma &= +1/2, & \Omega &= +3/2; \\ \Lambda &= -1, & \Sigma &= -1/2, & \Omega &= -3/2; \\ \Lambda &= +1, & \Sigma &= -1/2, & \Omega &= +1/2; \\ \Lambda &= -1, & \Sigma &= +1/2, & \Omega &= -1/2. \end{aligned} \tag{1.63}$$

The occurrence of $\Lambda = \pm 1$ is called Λ-doubling or Λ-degeneracy; in addition, the spin coupling gives rise to an additional two-fold doubling. The states with $|\Omega| = 3/2$ or $1/2$ are called fine-structure states, with spin–orbit energies $+A/2$ and $-A/2$ respectively; the value of $|\Omega|$ is written as a subscript in the state label. Hence we have $^2\Pi_{3/2}$ and $^2\Pi_{1/2}$ fine-structure components; if A is negative the $^2\Pi_{3/2}$ state is the lower in energy, and we have an 'inverted' doublet, the opposite case being called a 'regular' doublet. The NO molecule has a $^2\Pi_{1/2}$ ground state (regular), whilst the OH radical has a $^2\Pi_{3/2}$ ground state (inverted).

The rigid body rotational Hamiltonian can be written in the form

$$\begin{aligned}\mathcal{H}_{\rm rot} &= B\boldsymbol{R}^2 = B(\boldsymbol{J}-\boldsymbol{L}-\boldsymbol{S})^2\\ &= B(\boldsymbol{J}^2+\boldsymbol{L}^2+\boldsymbol{S}^2-2\boldsymbol{J}\cdot\boldsymbol{L}-2\boldsymbol{J}\cdot\boldsymbol{S}+2\boldsymbol{L}\cdot\boldsymbol{S}).\end{aligned} \tag{1.64}$$

The expansion of (1.64) is discussed in detail in chapter 8, and elsewhere, so we present only a brief and simplified summary here. Expanded in the molecule-fixed axis system, the diagonal part of the expression gives the result:

$$E_{\rm rot}(J) = B\{J(J+1)+S(S+1)+2\Lambda\Sigma+\Lambda^2-2\Omega^2\}. \tag{1.65}$$

There is, therefore, a sequence of rotational levels, characterised by their J values, for each fine-structure state. According to the discussion above, each J level has a two-fold degeneracy, forming what are called Ω-doublets or Λ-doublets. The off-diagonal ($q=\pm1$) terms from (1.64), together with the off-diagonal components of the spin–orbit coupling operator (1.62), remove the degeneracy of the Λ-doublets. The resulting pattern of the lower rotational levels for the OH radical is shown in figure 1.8, which is discussed in more detail in chapters 8 and 9. Transitions between the rotational levels, shown in the diagram, have been observed by far-infrared laser magnetic resonance, and transitions between the Λ-doublet components of the same rotational level have been observed by microwave rotational spectroscopy, by microwave magnetic resonance, by molecular beam maser spectroscopy, and by radio-astronomers studying interstellar gas clouds.

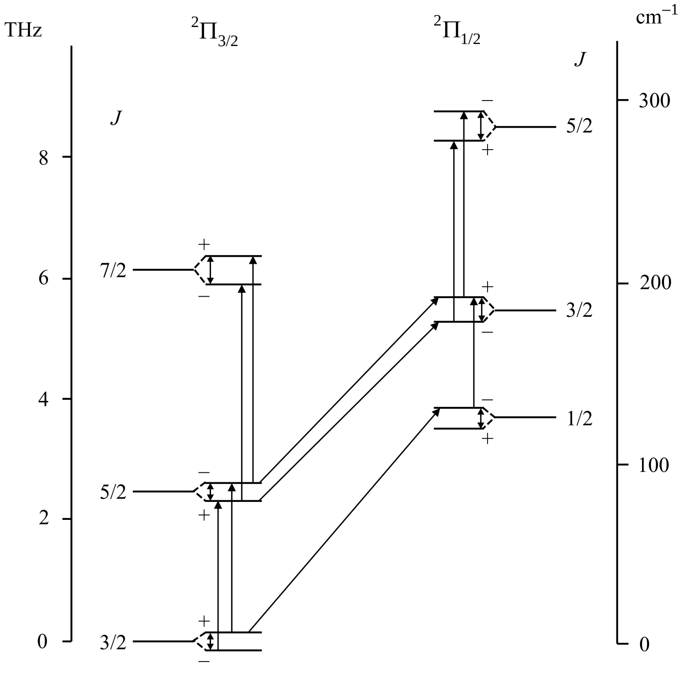

Figure 1.8. Lower rotational levels of the OH radical, and some of the transitions that have been observed. The size of the Λ-doublet splitting is exaggerated for the sake of clarity.

Interactions with an applied magnetic field are particularly important for open shell free radicals, many with $^2\Pi$ ground states having been studied by magnetic resonance methods. The Zeeman Hamiltonian may be written as the sum of four terms:

$$\begin{aligned}\mathcal{H}_Z = {} & g_L \mu_B \mathrm{T}^1(\boldsymbol{B}) \cdot \mathrm{T}^1(\boldsymbol{L}) + g_S \mu_B \mathrm{T}^1(\boldsymbol{B}) \cdot \mathrm{T}^1(\boldsymbol{S}) - g_N \mu_N \mathrm{T}^1(\boldsymbol{B}) \cdot \mathrm{T}^1(\boldsymbol{I}) \\ & - g_r \mu_B \mathrm{T}^1(\boldsymbol{B}) \cdot \{\mathrm{T}^1(\boldsymbol{J}) - \mathrm{T}^1(\boldsymbol{L}) - \mathrm{T}^1(\boldsymbol{S})\}. \end{aligned} \tag{1.66}$$

All of these terms must be included in an accurate analysis and their effects are described in detail in chapter 9. The most important terms, however, are the first two. Putting the orbital g-factor, g_L, equal to 1 one can show that for a good case (a) molecule the effective g-value for the rotational level J is

$$g_J = \frac{(\Lambda + \Sigma)(\Lambda + g_S \Sigma)}{J(J+1)}. \tag{1.67}$$

If we put $g_S = 2$, we find that for the lowest rotational level of the $^2\Pi_{3/2}$ state, $J = 3/2$, the g-factor is $4/5$. For any rotational level of the $^2\Pi_{1/2}$ state, however, (1.67) predicts a g-factor of zero. For a perfect case (a) molecule, therefore, we cannot use magnetic resonance methods to study $^2\Pi_{1/2}$ states. Fortunately perhaps, most molecules are intermediate between case (a) and case (b) so that both fine-structure states are magnetic to some extent. The other point to notice from (1.67) is that the g-factor decreases rapidly as J increases.

We will see elsewhere is this book many examples of the spectra of $^2\Pi$ molecules. We will see also that although our discussion above is based upon a case (a) coupling scheme for the various angular momenta, case (b) is often just as appropriate and, as we have already noted, many molecules are really intermediate between case (a) and case (b). We will also meet electronic states with higher spin and orbital multiplicity. For $S \geq 1$, the terms describing the interaction between electron spins play much the same role in Π and Δ states as they do for Σ states. Nuclear hyperfine interactions are also similar to those described already, with the addition of an orbital hyperfine term which may be written in the form

$$\mathcal{H}_{\mathrm{IL}} = a \mathrm{T}^1(\boldsymbol{I}) \cdot \mathrm{T}^1(\boldsymbol{L}), \tag{1.68}$$

where the orbital hyperfine constant is given by

$$a = 2 \mu_B g_N \mu_N (\mu_0 / 4\pi) \langle r^{-3} \rangle; \tag{1.69}$$

r is the distance between the nucleus and the orbiting electron, with the average calculated from a suitable electronic wave function.

The purpose of this section has been to introduce the complexity in the sub-structure of rotational levels, and the richness of the consequent spectroscopy which is revealed by high-resolution techniques. Understanding the origin and details of this structure also takes us very deeply into molecular quantum mechanics, as we show in chapters 2 to 7.

1.7. The effective Hamiltonian

The process of analysing a complex diatomic molecule spectrum with electron spin, nuclear hyperfine and external field interactions has several stages. We need to derive expressions for the energies of the levels involved, which means choosing a suitable basis set and a suitable ‘effective Hamiltonian’. The best basis set is that particular Hund’s case which seems the nearest or most convenient approximation to the ‘truth’. The effective Hamiltonian is a sum of terms representing the various interactions within the molecule; each term contains angular momentum operators and ‘molecular parameters’. Our choice of effective Hamiltonian is also determined by the basis set chosen. The procedure is then to set up a matrix of the effective Hamiltonian operating within the chosen basis. The matrix is often truncated artificially, and we then diagonalise the matrix to obtain the energies of the levels and the effective wave functions. Armed with this information we attempt to assign the lines in the spectrum. The spectral frequencies are expressed in terms of the molecular parameters, and usually a first set of values is determined. If the assignment is correct, a program designed to minimise the differences between calculated and measured transition frequencies is employed. The final best values of the molecular parameters may then be used for comparison with the predictions of electronic structure calculations. In this way we hope to develop a better description of the electronic structure of the molecule.

The choice of the effective Hamiltonian is often far from straightforward; indeed we have devoted a whole chapter to this subject (chapter 7). In this section we give a gentle introduction to the problems involved, and show that the definition of a particular ‘molecular parameter’ is not always simple. The problem we face is not difficult to understand. We are usually concerned with the sub-structure of one or two rotational levels at most, and we aim to determine the values of the important parameters relating to those levels. However, these parameters may involve the participation of other vibrational and electronic states. We do *not* want an effective Hamiltonian which refers to other electronic states explicitly, because it would be very large, cumbersome and essentially unusable. We want to analyse our spectrum with an effective Hamiltonian involving *only* the quantum numbers that arise directly in the spectrum. The effects of all other states, and their quantum numbers, are to be absorbed into the definition and values of the ‘molecular parameters’. The way in which we do this is outlined briefly here, and thoroughly in chapter 7.

The development of the effective Hamiltonian has been due to many authors. In condensed phase electron spin magnetic resonance the so-called ‘spin Hamiltonian’ [20, 21] is an example of an effective Hamiltonian, as is the ‘nuclear spin Hamiltonian’ [22] used in liquid phase nuclear magnetic resonance. In gas phase studies, the first investigation of a free radical by microwave spectroscopy [23] introduced the ideas of the effective Hamiltonian, as also did the first microwave magnetic resonance study [24]. Miller [25] was one of the first to develop the more formal aspects of the subject, particularly so far as gas phase studies are concerned, and Carrington, Levy and Miller [26] have reviewed the theory of microwave magnetic resonance, and the use of the effective Hamiltonian.

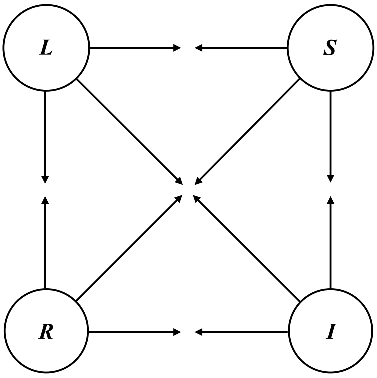

Figure 1.9. Possible pairwise interactions of $\boldsymbol{L}$, $\boldsymbol{S}$, $\boldsymbol{R}$ and $\boldsymbol{I}$.

As a simple introduction to the subject [27], let us consider the four angular momentum vectors illustrated in figure 1.9. They are as follows:

$\boldsymbol{R}$: the rotational angular momentum of the bare nuclei,
$\boldsymbol{L}$: the electronic orbital angular momentum,
$\boldsymbol{S}$: the electronic spin angular momentum,
$\boldsymbol{I}$: the nuclear spin angular momentum.

Each angular momentum can interact with the other three, and figure 1.9 draws attention to the following pairwise interactions:

$(\boldsymbol{L})(\boldsymbol{S})$: spin–orbit coupling,
$(\boldsymbol{L})(\boldsymbol{R})$: rotational–electronic interaction,
$(\boldsymbol{L})(\boldsymbol{I})$: hyperfine interaction between the electron orbital and nuclear spin magnetic moments,
$(\boldsymbol{S})(\boldsymbol{I})$: hyperfine interaction between the electron and nuclear spin magnetic moments,
$(\boldsymbol{S})(\boldsymbol{R})$: interaction between the electron spin and rotational magnetic moments,
$(\boldsymbol{I})(\boldsymbol{R})$: interaction between the nuclear spin and rotational magnetic moments.

The direct interactions listed above and illustrated in figure 1.9 can occur in the effective Hamiltonian, but figure 1.10 shows how the effective Hamiltonian can also contain similar terms which arise indirectly. In figure 1.10(a) we illustrate the interaction of $\boldsymbol{R}$ with $\boldsymbol{L}$, which in turn couples with the spin $\boldsymbol{S}$. Consequently the effective Hamiltonian may contain a term of the form $(\boldsymbol{R})(\boldsymbol{S})$, part of which arises from the direct coupling shown in figure 1.9, but with the remaining part coming from the indirect coupling via $\boldsymbol{L}$. If we are dealing with a diatomic molecule in a Σ state, there is no first-order orbital angular momentum, but the spin–orbit coupling can mix the ground state with one or more excited Π states, thereby generating some orbital angular momentum in the ground state [28]. Consequently the spin–rotation constant γ comprises a first-order direct contribution, plus a second-order contribution arising from admixture of excited states. In all but the lightest molecules, this second-order contribution is the largest in magnitude.

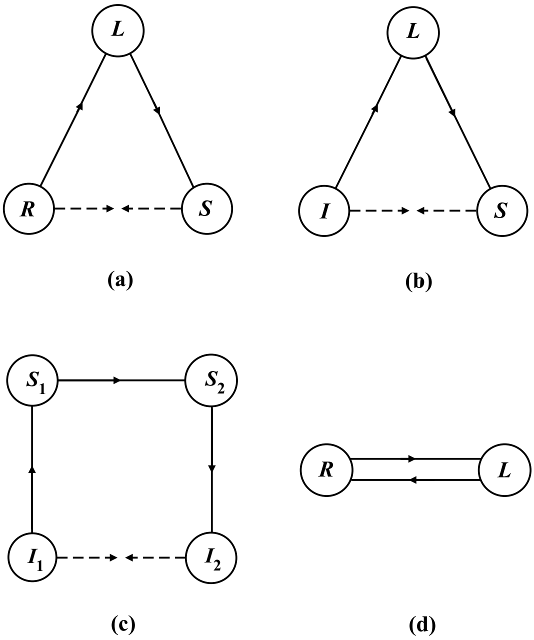

Figure 1.10. (a) Second-order spin–rotation interaction occurring via $\boldsymbol{L}$. (b) Second-order pseudo-contact hyperfine interaction occurring via $\boldsymbol{L}$. (c) Electron coupled nuclear spin–spin interaction. (d) Second-order interaction of $\boldsymbol{R}$ and $\boldsymbol{L}$.

Another example is the pseudo-contact hyperfine interaction illustrated in figure 1.10(b); spin–orbit mixing of excited Π states with a Σ ground state generates orbital angular momentum in the ground state, which interacts with the nuclear spin magnetic moment. Overall, therefore, the interaction looks somewhat like a direct Fermi contact interaction, $\boldsymbol{S} \cdot \boldsymbol{I}$. A third example, illustrated in figure 1.10(c), involves two electron spins ($\boldsymbol{S}_1$ and $\boldsymbol{S}_2$) and two nuclear spins ($\boldsymbol{I}_1$ and $\boldsymbol{I}_2$). The nuclear spin $\boldsymbol{I}_1$ interacts with the electron spin $\boldsymbol{S}_1$; $\boldsymbol{S}_1$ is coupled with $\boldsymbol{S}_2$, which in turn interacts with $\boldsymbol{I}_2$. The net result is an interaction which is represented in the effective Hamiltonian by a term of the form $\boldsymbol{I}_1 \cdot \boldsymbol{I}_2$. This interaction is called the 'electron-coupled nuclear spin–spin interaction', and it is the origin of the spin–spin splittings observed in liquid phase nuclear magnetic resonance spectra. Note that it is not necessary for the total spin $\boldsymbol{S} = \boldsymbol{S}_1 + \boldsymbol{S}_2$ to be non-zero; the interaction can and does occur in closed shell molecules.

Our final example, illustrated in figure 1.10(d), involves the rotational angular momentum $\boldsymbol{R}$ and the orbital angular momentum $\boldsymbol{L}$. The second-order effect of the coupling for a ground $^1\Sigma$ state, operating through admixture of excited states, involves the product of matrix elements containing the operator products $(\boldsymbol{R} \cdot \boldsymbol{L})(\boldsymbol{R} \cdot \boldsymbol{L})$. The net effect is a term in the effective Hamiltonian which contains the operator $\boldsymbol{R}^2$. Remembering that the rotational angular momentum of the nuclei is also represented in the effective Hamiltonian by a term $B\boldsymbol{R}^2$, we see that the rotational constant B must be interpreted with some care, because it contains a very small contribution from the electrons, added to the major contribution of the nuclei.

Many different procedures for reducing the complete Hamiltonian to a suitable effective Hamiltonian have been devised. These are reviewed in detail in chapter 7; we will see that the methods involve different forms of perturbation theory [29].

1.8. Bibliography

The subject matter of this book is scattered between many other books, and much of it does not yet appear in any book. The most important book which deals exclusively with diatomic molecules is that by Herzberg [4], combined with the later supplement by Huber and Herzberg [13] which lists data up to 1979. This takes us into the era of computerised data bases (see below), which are the best sources for numerical data, and are the reason why we have made no attempt at a comprehensive data coverage in this book. A further important book is that by Lefebvre-Brion and Field [29]; the title of this book suggests a rather specialised treatment but it is actually both wide and deep in its coverage. Other books which deal specifically with theoretical aspects of diatomic molecules are those by Judd [30], dealing with angular momentum theory, Kovács [31] and Mizushima [32]. Angular momentum theory occupies a central position in understanding the energy levels of both diatomic and polyatomic molecules. In this book we use the methods and conventions of Edmonds [33], but have also benefited from the reader-friendly accounts provided by Rose [34], Zare [35] and Brink and Satchler [36]. Quantum mechanics is the fundamental theory which must be mastered if molecular spectroscopy is to be understood. This is not the place for a comprehensive listing of the many books on this subject, but we have found the books by Flygare [2], Moss [37] and Hannabuss [38] to be helpful; in particular, our treatment of relativistic quantum mechanics in chapters 3 and 4 owes much to those by Moss and Hannabuss. The book by Bunker and Jensen [39] is our standard source for problems involving symmetry and group theory.

Molecular beams are important in this book. For the early work the book by Ramsey [3] is indispensable, and a recent two-volume comprehensive survey edited by Scoles [40] covers recent developments in the technology. However, books dealing with microwave, millimetre wave or far-infrared spectroscopy, whether using beams or not, are scarce. The early books of Townes and Schawlow [41], Kroto [42] and Carrington [27] still have some value, and more recently Hirota [43] has described spectroscopic work (mainly Japanese) on transient molecules. There is, however, a vast amount of published original work on the high-resolution spectroscopy of transient species, using far-infrared or lower radiation frequencies. This book is devoted to a description of this type of work applied to diatomic molecules. More general books on molecular spectroscopy, including diatomic molecules, are those by Hollas [44], Demtröder [45] and Bernath [46]. In the field of radio astronomy we have found the book by Rohlfs and Wilson [47] to be most helpful.

There are, of course, a number of review articles from which we select three, all written by Hirota and all dealing with free radicals and molecular ions. The first of these covers the period up to 1992 [48] and deals with diatomic and polyatomic species. It is supplemented by further reviews published in 1994 [49] and 2000 [50]. Finally we should draw attention to a computer data base covering all types of spectroscopy of diatomic molecules, produced by Bernath and McLeod [51]. This is available free of charge on the Internet and may be seen at <http://diref.uwaterloo.ca>. It will be maintained for the indefinite future.

Appendix 1.1. Maxwell's equations

An important connection between optical and electromagnetic phenomena was first discovered by Faraday in 1846. He observed that when plane-polarised radiation passes through certain materials exposed to a magnetic field that is parallel to the propagation direction of the radiation, the plane of polarisation is rotated. The degree of rotation depends upon the nature of the material and the strength of the magnetic field. The union of optical and electromagnetic properties was subsequently put on firm foundations by Maxwell in the form of his wave theory of electromagnetic interactions. As we shall see, Maxwell's equations also provide the explanation for optical properties like dispersion and refraction. The nature of electromagnetic radiation, which is central to almost everything in this book, was described earlier in this chapter, but without much justification. Maxwell's equations, which form the basis for understanding electromagnetic radiation, will now be described. There are, in fact, four equations that connect macroscopic electric and magnetic phenomena, and two further equations that describe the response of a material medium to electric and magnetic fields.

(i) The first equation is

$$\begin{aligned} \nabla \wedge \boldsymbol{E} + \frac{1}{c}\frac{\partial \boldsymbol{B}}{\partial t} &= 0 \quad \text{(in cgs units)}, \\ \nabla \wedge \boldsymbol{E} + \frac{\partial \boldsymbol{B}}{\partial t} &= 0 \quad \text{(in SI units)}. \end{aligned} \tag{1.70}$$

∇ is the vector operator given by

$$\nabla = \boldsymbol{i}\frac{\partial}{\partial x} + \boldsymbol{j}\frac{\partial}{\partial y} + \boldsymbol{k}\frac{\partial}{\partial z}, \tag{1.71}$$

where $\boldsymbol{i}$, $\boldsymbol{j}$, $\boldsymbol{k}$ are orthogonal unit vectors. When ∇ operates on a scalar ϕ the resulting vector $\nabla\phi$ is called the gradient of ϕ (i.e. grad ϕ). When ∇ operates on a vector $\boldsymbol{A}$ there are two possibilities. The scalar product, $\nabla \cdot \boldsymbol{A}$, results in a new scalar, and is known as the divergence of $\boldsymbol{A}$ (i.e. div $\boldsymbol{A}$). The vector product, $\nabla \wedge \boldsymbol{A}$, is a vector called the curl of $\boldsymbol{A}$; c, as elsewhere, is the speed of light.

Equation (1.70) is Faraday's law of electromagnetic induction; it shows that a time-dependent magnetic flux density, $\boldsymbol{B}$, gives rise to an electric field, $\boldsymbol{E}$, in a direction perpendicular to the original magnetic field. Equations (1.70) are often written in the abbreviated form

$$\begin{aligned} \mathrm{curl}\boldsymbol{E} + \frac{1}{c}\frac{\partial \boldsymbol{B}}{\partial t} &= 0 \quad \text{(in cgs units)}, \\ \mathrm{curl}\boldsymbol{E} + \frac{\partial \boldsymbol{B}}{\partial t} &= 0 \quad \text{(in SI units)}. \end{aligned} \tag{1.72}$$

(ii) The second equation is

$$\begin{aligned} \nabla \wedge \boldsymbol{H} - \frac{1}{c}\frac{\partial \boldsymbol{D}}{\partial t} &= \frac{4\pi}{c}\boldsymbol{J} \quad \text{(in cgs units)}, \\ \nabla \wedge \boldsymbol{H} - \frac{\partial \boldsymbol{D}}{\partial t} &= \boldsymbol{J} \qquad \text{(in SI units)}. \end{aligned} \tag{1.73}$$

H is the magnetic field vector and ***D*** is called the electric induction or displacement field. This equation is known as the Ampere–Oersted law and shows that a magnetic field will exist near an electric current density ***J***. The displacement field, ***D***, is necessary to propagate electromagnetic energy through space. ***J*** has units charge $\cdot$ area$^{-1} \cdot$ t^{-1}

(iii) The third equation is

$$\begin{aligned} \nabla \cdot \boldsymbol{D} &= 4\pi\bar{\rho} \quad \text{(in cgs units)}, \\ \nabla \cdot \boldsymbol{D} &= \bar{\rho} \qquad \text{(in SI units)}. \end{aligned} \tag{1.74}$$

$\nabla \cdot$ is called the div and $\bar{\rho}$ is the electric charge density with units charge $\cdot$ volume^{-1}. There is a relationship between ***J*** and $\bar{\rho}$, given by

$$\boldsymbol{J} = \bar{\rho}\mathbf{v}, \tag{1.75}$$

where **v** is the velocity of the charge distribution. ***J*** and ***E*** are also related by

$$\boldsymbol{J} = \boldsymbol{\sigma} \cdot \boldsymbol{E}, \tag{1.76}$$

where $\boldsymbol{\sigma}$ is the conductivity. Equation (1.74) is actually the Coulomb law in electrostatics.

(iv) The fourth equation is the same in both cgs and SI units, and is

$$\nabla \cdot \boldsymbol{B} = 0. \tag{1.77}$$

This equation states that there are no sources of magnetic field except currents; in other words, there are no free magnetic poles.

The remaining two equations both relate to properties of the medium.

(v) The fifth equation may be written

$$\begin{aligned} \boldsymbol{D} &= \boldsymbol{\varepsilon} \cdot \boldsymbol{E} \qquad \text{(in cgs units)}, \\ \boldsymbol{D} &= \varepsilon_0 \boldsymbol{\varepsilon} \cdot \boldsymbol{E} \quad \text{(in SI units)}. \end{aligned} \tag{1.78}$$

$\boldsymbol{\varepsilon}$ is the relative electric permittivity, or dielectric constant, of the medium, expressed in general as a tensor, and ε_0 is the permittivity of a vacuum.

(vi) The sixth equation is the magnetic analogue of the fifth:

$$\begin{aligned} \boldsymbol{B} &= \boldsymbol{\mu}_p \cdot \boldsymbol{H} && \text{(in cgs units)}, \\ \boldsymbol{B} &= \mu_0 \boldsymbol{\mu}_p \cdot \boldsymbol{H} && \text{(in SI units)}. \end{aligned} \tag{1.79}$$

$\boldsymbol{B}$ is the magnetic induction or magnetic flux density, and $\boldsymbol{\mu}_p$ is the relative magnetic permeability of the medium, also expressed in general as a tensor. For an anisotropic medium the scalars ε and μ_p are used; their values are unity for a vacuum (so that $\boldsymbol{B}$ and $\boldsymbol{H}$ are then equivalent). ε has a wide range of values for different substances, but μ_p is usually close to unity. If μ_p is less than 1.0 the substance is diamagnetic, and if it is greater than 1.0 the substance is paramagnetic.

The permittivity of a vacuum is

$$\varepsilon_0 = 8.854\,187\,818 \times 10^{-12}\,\text{s}^4\,\text{A}^2\,\text{kg}^{-1}\,\text{m}^{-3}, \tag{1.80}$$

and the permeability of free space is

$$\mu_0 = 4\pi \times 10^{-7}\,\text{kg}\,\text{m}\,\text{s}^{-2}\,\text{A}^{-2}. \tag{1.81}$$

It also follows from the above equations that

$$(1/\varepsilon_0\mu_0)^{1/2} = c. \tag{1.82}$$

Appendix 1.2. Electromagnetic radiation

The oscillating electric and magnetic fields of a plane wave, shown in figure 1.2, may be represented by the following simple equations:

$$\begin{aligned} \boldsymbol{E} &= \boldsymbol{k} E_0 \sin(Y - \mathrm{v}t), \\ \boldsymbol{B} &= \boldsymbol{i} B_0 \sin(Y - \mathrm{v}t), \end{aligned} \tag{1.83}$$

in which E_0, B_0 and v are simply constants. We now show that this electromagnetic field satisfies Maxwell's equations provided certain conditions are met. We find the following results:

$$\begin{aligned} \operatorname{div} \boldsymbol{E} &= 0, \\ \operatorname{curl} \boldsymbol{E} &= \boldsymbol{i} \frac{\partial E_Z}{\partial Y} = \boldsymbol{i} E_0 \cos(Y - \mathrm{v}t) \\ \frac{\partial \boldsymbol{E}}{\partial t} &= -\mathrm{v} \boldsymbol{k} E_0 \cos(Y - \mathrm{v}t). \end{aligned} \tag{1.84}$$

$$\begin{aligned} \operatorname{div} \boldsymbol{B} &= 0, \\ \operatorname{curl} \boldsymbol{B} &= -\boldsymbol{k} \frac{\partial B_X}{\partial Y} = -\boldsymbol{k} B_0 \cos(Y - \mathrm{v}t), \\ \frac{\partial \boldsymbol{B}}{\partial t} &= -\mathrm{v} \boldsymbol{i} B_0 \cos(Y - \mathrm{v}t). \end{aligned} \tag{1.85}$$

We note also that $\boldsymbol{J} = 0$ in empty space. If these results are combined with (1.72) and (1.73), the conditions that must be satisfied are, in SI units,

$$E_0 = \mathrm{v}B_0, \qquad B_0 = \mu_0\varepsilon_0\mathrm{v}E_0. \tag{1.86}$$

Taken together, these equations require that

$$\mathrm{v} = \pm c, \qquad E_0 = cB_0. \tag{1.87}$$

In the old cgs units, the second relationship is even simpler:

$$E_0 = B_0. \tag{1.88}$$

We have therefore established three important features of the electromagnetic radiation. The first is that the field pattern travels with the speed of light, c. The second is that at every point in the wave at any instant of time, the electric and magnetic field strengths are directly related to each other. The third is that the electric and magnetic fields are perpendicular to one another, and to the direction of travel.

References

[1] E.M. Purcell, *Electricity and Magnetism*, McGraw-Hill Book Company, Singapore, 1985.

[2] W.H. Flygare, *Molecular Structure and Dynamics*, Prentice-Hall, Inc., New Jersey, 1978.

[3] N.F. Ramsey, *Molecular Beams*, Oxford University Press, Oxford, 1956.

[4] G. Herzberg, *Spectra of Diatomic Molecules*, D. Van Nostrand Company, Inc., Princeton, 1950.

[5] W. Gordy, *Rev. Mod. Phys.*, **20**, 668 (1948).

[6] J.P. Cooley and J.H. Rohrbaugh, *Phys. Rev.*, **67**, 296 (1945).

[7] R.T. Weidner, *Phys. Rev.*, **72**, 1268 (1947); **73**, 254 (1948).

[8] C.H. Townes, F.R. Merritt and B.D. Wright, *Phys. Rev.*, **73**, 1334 (1948).

[9] R. Beringer, *Phys. Rev.*, **70**, 53 (1946).

[10] R. Beringer and J.G. Castle, *Phys. Rev.*, **75**, 1963 (1949); **76**, 868 (1949).

[11] J.M.B. Kellogg, I.I. Rabi, N.F. Ramsey and J.R. Zacharias, *Phys. Rev.*, **56**, 728 (1939).

[12] H.K. Hughes, *Phys. Rev.*, **72**, 614 (1947).

[13] K.P. Huber and G. Herzberg, *Constants of Diatomic Molecules*, Van Nostrand Reinhold Company, New York, 1979.

[14] D.R. Lide, *J. Chem. Phys.*, **38**, 2027 (1963).

[15] F. Hund, *Z. Physik*, **42**, 93 (1927).

[16] J.H. Van Vleck, *Phys. Rev.*, **33**, 467 (1929).

[17] H.A. Kramers, *Z. Physik*, **53**, 422 (1929).

[18] R. Schlapp, *Phys. Rev.*, **51**, 342 (1937).

[19] D. De Santis, A. Lurio, T.A. Miller and R.S. Freund, *J. Chem. Phys.*, **58**, 4625 (1973).

[20] A. Abragam and B. Bleaney, *Electron Paramagnetic Resonance of Transition Ions*, Clarendon Press, Oxford, 1970.

[21] A. Carrington and A.D. McLachlan, *Introduction to Magnetic Resonance*, Harper and Row, New York, 1967.

[22] J.A. Pople, W.G. Schneider and H.J. Bernstein, *High-resolution Nuclear Magnetic Resonance*, McGraw-Hill Book Company, Inc., New York, 1959.

[23] G.C. Dousmanis, T.M. Sanders and C.H. Townes, *Phys. Rev.*, **100**, 1735 (1955).

[24] H.E. Radford, *Phys. Rev.*, **126**, 1035 (1962).

[25] T.A. Miller, *Mol. Phys.*, **16**, 105 (1969).

[26] A. Carrington, D.H. Levy and T.A. Miller, *Adv. Chem. Phys.*, **18**, 149 (1970).

[27] A. Carrington, *Microwave Spectroscopy of Free Radicals*, Academic Press, London, 1974.

[28] J.H. Van Vleck, *Rev. Mod. Phys.*, **23**, 213 (1951).

[29] H. Lefebvre-Brion and R.W. Field, *Perturbations in the Spectra of Diatomic Molecules*, Academic Press, Inc., Orlando, 1986.

[30] B.R. Judd, *Angular Momentum Theory for Diatomic Molecules*, Academic Press, Inc., New York, 1975.

[31] I. Kovács, *Rotational Structure in the Spectra of Diatomic Molecules*, Adam Hilger Ltd., London, 1969.

[32] M. Mizushima, *The Theory of Rotating Diatomic Molecules*, John Wiley and Sons, New York, 1975.

[33] A.R. Edmonds, *Angular Momentum in Quantum Mechanics*, Princeton University Press, Princeton, 1960.

[34] M.E. Rose, *Elementary Theory of Angular Momentum*, John Wiley and Sons, Inc., New York, 1957.

[35] R.N. Zare, *Angular Momentum*, John Wiley and Sons, New York, 1988.

[36] D.M. Brink and G.R. Satchler, *Angular Momentum*, Clarendon Press, Oxford, 1962.

[37] R.E. Moss, *Advanced Molecular Quantum Mechanics*, Chapman and Hall, London, 1973.

[38] K. Hannabuss, *An Introduction to Quantum Theory*, Oxford University Press, 1997.

[39] P.R. Bunker and P. Jensen, *Molecular Symmetry and Spectroscopy*, NRC Research Press, Ottawa, 1998.

[40] *Atomic and Molecular Beam Methods*, ed. G. Scoles, Oxford University Press, New York, 1988.

[41] C.H. Townes and A.L. Schawlow, *Microwave Spectroscopy*, McGraw-Hill Book Company, New York, 1955.

[42] H.W. Kroto, *Molecular Rotation Spectra*, John Wiley and Sons, London, 1975.

[43] E. Hirota, *High-resolution Spectroscopy of Transient Molecules*, Springer-Verlag, Berlin, 1985.

[44] J.M. Hollas, *Modern Spectroscopy*, John Wiley and Sons, Ltd., Chichester, 1996.

[45] W. Demtröder, *Laser Spectroscopy*, Springer-Verlag, Berlin, 1982.

[46] P.F. Bernath, *Spectra of Atoms and Molecules*, Oxford University Press, New York, 1995.

[47] K. Rohlfs and T.L. Wilson, *Tools of Radio Astronomy (Third Edition)*, Springer-Verlag, Berlin, 2000.

[48] E. Hirota, *Chem. Rev.*, **92**, 141 (1992).

[49] E. Hirota, *Ann. Rep. Prog. Chem., Sect. C*, **91**, 3 (1994).

[50] E. Hirota, *Ann. Rep. Prog. Chem., Sect. C*, **96**, 95 (2000).

[51] P.F. Bernath and S.McLeod, *DiRef – A Database of References Associated with the Spectra of Diatomic Molecules*, University of Waterloo Chemical Physics report.